LA-6675-PR
Progress Report

UC-15
Issued: January 1977

Nuclear Safeguards Research

Program Status Report

May—August 1976

by

Nuclear Safeguards Research Group, R-1
Nuclear Safeguards, Reactor Safety and Technology Division

los alamos
scientific laboratory
of the University of California
LOS ALAMOS, NEW MEXICO 87545

An Affirmative Action/Equal Opportunity Employer

UNITED STATES
ENERGY RESEARCH AND DEVELOPMENT ADMINISTRATION
CONTRACT W-7405-ENG. 36

The four most recent reports in this series, unclassified, are LA-6040-PR, LA-6142-PR, LA-6316-PR, and LA-6530-PR.

This work was supported by the Division of Safeguards and Security, US Energy Research and Development Administration.

Printed in the United States of America. Available from
National Technical Information Service
U.S. Department of Commerce
5285 Port Royal Road
Springfield, VA 22161
Price: Printed Copy $4.50 Microfiche $3.00

ABSTRACT

This report presents the status of the two Nondestructive Assay Research and Development programs pursued by the LASL Nuclear Safeguards Research Group R-1 during the period May-August 1976. Salient topics of the two programs are summarized in the table of contents.

CONTENTS

PART I
NUCLEAR MATERIAL SAFEGUARDS PROGRAM— NONDESTRUCTIVE ASSAY TECHNIQUES

I. NONDESTRUCTIVE ASSAY APPLICATIONS AND RESULTS

A. Assay of Uranium-Thorium Mixtures with the Van de Graaff Small Sample Assay Station (M. S. Krick)

The Van de Graaff small sample assay station (SSAS) previously described[1] normally uses 400-600 keV source neutrons to induce fissions in fissile materials to perform assays by delayed-neutron counting. In principle, mixtures of fissile and fertile materials can be assayed for both the fissile and fertile components by irradiating the samples with neutrons whose energies are below the fission thresholds to measure the fissile component and then by repeating the measurements with neutrons whose energies are above these thresholds to determine the fertile component.

To investigate the usefulness of this technique, uranium-thorium mixtures containing 93.18%-enriched uranium were assayed for ^{235}U and ^{232}Th content. Neutrons with energies of 400-600 keV were used to induce fissions in ^{235}U and neutrons with energies of 1.6-1.8 MeV were used to induce fissions in ^{235}U, ^{238}U, and ^{232}Th. The $^{7}Li(p,n)$ reaction was used to produce the neutrons in both cases. Because the enrichment of the uranium was assumed to be 93.18% for all samples, the masses of uranium and thorium (m_U and m_T, respectively) in the samples could be determined approximately from the simple equations

$$R^{\ell} = R^{\ell}_{U}\, m_U$$

$$R^{h} = R^{h}_{U}\, m_U + R^{h}_{T}\, m_T \ .$$

R^{ℓ} and R^{h} are the responses of the SSAS to low energy (400-600 keV) and high energy (1.6-1.8 MeV) neutron interrogations, respectively. R^{ℓ}_{U}, R^{h}_{U}, and R^{h}_{T} are the SSAS responses per unit mass for uranium at low energy, uranium at high energy, and thorium at high energy, respectively. Small response nonlinearities (due, for example, to multiplication or geometric effects[2]) were ignored.

The samples used in this experiment were prepared by LASL Group CMB-1; the composition of the samples is detailed in Table I. Samples 51 (uranium only) and 28, 53, and 54 (thorium only) were used as standards in this experiment for the assay of samples 26, 57, and 60 (mixed uranium and thorium). The calibration constants R^{ℓ}_{U}, R^{h}_{U}, and R^{h}_{T} determined from samples 51, 28, 53, and 54 and arbitrarily normalized were

$$R^{h}_{U} = 100.0$$
$$R^{\ell}_{U} = 93.6$$
$$R^{h}_{T} = 10.9 \ .$$

Tables II and III show the assay results for samples 26, 57, and 60 for ^{235}U and ^{232}Th content. The average magnitude of the deviation between the given mass and assayed mass is 1.4%. Because the standard deviations of the measurements of R^{ℓ} and R^{h} are about 1%, the agreement between the given masses and the assay masses is generally satisfactory.

This preliminary experiment demonstrates that the Van de Graaff SSAS can be used for both uranium and thorium assay in mixed uranium-thorium samples if the uranium enrichment is constant for all samples. The same technique should also be useful for determining the masses of ^{235}U and ^{238}U (i.e., for determining the uranium mass and enrichment) in small uranium samples containing assorted matrix materials.

TABLE I

URANIUM-THORIUM SAMPLE DATA

Sample Number	Mass (g)			Enrichment (%)
	Thorium	Uranium	^{235}U	
26	3.9998	0.9998	0.9316	93.18
28	4.001	0	—	—
51	0	0.5873	0.5472	93.18
53	11.9972	0	—	—
54	2.9704	0	—	—
57	3.0152	0.5966	0.5559	93.18
60	11.9905	0.6246	0.5820	93.18

B. Assay of Reprocessing Waste

1. Prototype for 55-gal Barrel Assay (T. W. Crane)

Standard 55-gal barrels will contain most of the waste generated at fuel reprocessing plants. In some cases fission product activity may be as high as 100 R/h at the barrel surface. Because of this intense gamma-ray activity and strong attenuation of the usual gamma-ray signatures (i.e., 414 keV for plutonium) neutron assay techniques will most likely be preferable. Of the available neutron NDA techniques, the three most practical for this application are: (a) coincidence counting of spontaneous fission neutrons, (b) subthreshold neutron interrogation with detection of prompt energetic fission neutrons, and (c) subthreshold neutron interrogation with delayed fission neutron counting. The success of these approaches will depend on the effectiveness of the gamma-ray shielding of the neutron counters and on the proper interpretation of matrix effects such as (α,n) reactions, hydrogenous material, and the presence of transuranic (TRU) isotopes (i.e., ^{242}Cm or ^{244}Cm). To date only the shielding has been considered in a quantitative way and its properties will be discussed in Sec. I-B-2.

Many passive coincidence counters have been built, including 4π counters large enough to accommodate 30- and 55-gal barrels (see Ref. 3, p. 18 and Ref. 4, p. 20). The performance of a system with gamma-ray shielding can be extrapolated from the

TABLE II

^{235}U ASSAY RESULTS

Sample Number	CMB-1 Mass (g)	Assay Mass (g)	Relative Difference[a] (%)
26	0.9316	0.9333	+0.2
57	0.5559	0.5495	−1.2
60	0.5820	0.5921	+1.7

[a]Relative differences are calculated with respect to the CMB-1 values.

TABLE III

^{232}Th ASSAY RESULTS

Sample Number	CMB-1 Mass (g)	Assay Mass (g)	Relative Difference[a] (%)
26	3.9998	3.814	−4.6
57	3.0152	3.008	−0.2
60	11.9905	11.962	−0.2

[a]Relative differences are calculated with respect to the CMB-1 values.

behavior of existing counters with perhaps only minor modifications for test measurements. Considerably less data are available for the active interrogation of 55-gal barrels by isotopic neutron sources. To evaluate this approach, we plan to add an assay chamber capable of accommodating 55-gal barrels to the Shuffler system (see Ref. 5, p. 25) as shown in Fig. 1. The feasibility of using a ^{252}Cf interrogation source for delayed neutron counting of large, highly radioactive samples will be tested. Later a photoneutron source (e.g., ^{124}Sb-Be or Ra-Be) with ^{4}He detectors will be used to investigate the subthreshold neutron interrogation with detection of prompt energetic neutrons.

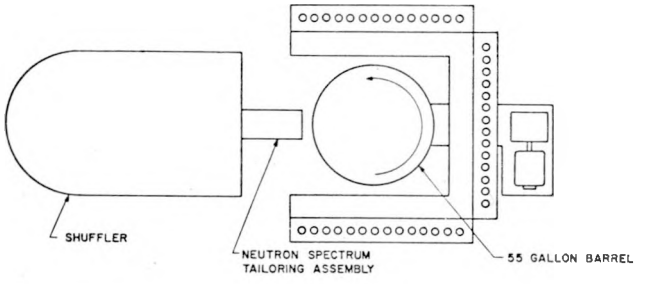

(a) Top view.

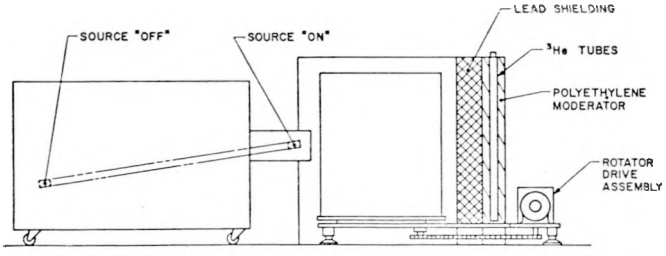

(b) Side view.

Fig. 1.
Test setup for assaying 55-gal barrels by delayed fission neutron counting using the ^{252}Cf Shuffler.

2. Shielding for ^{3}He Detectors (T. W. Crane)

The ^{3}He proportional tubes are efficient neutron detectors up to the point where the pile-up pulses from intense gamma-ray radiation exceed the threshold set for neutrons. This pile-up effect has been investigated for ^{4}He tubes (see Ref. 6, p. 24 and Ref. 7, p. 6). The gamma-ray pile up for a ^{3}He tube is shown in Fig. 2. The degradation of the neutron signal with increasing gamma dose rate can be clearly seen. For the ^{3}He tube tested, the maximum radiation level at which neutrons can still be reliably detected is about 4 R/h. At this radiation level a preamplifier,[8] amplifier, and single channel analyzer are required for each tube. Because the test setup uses 54 tubes, a sizable electronics array is required.

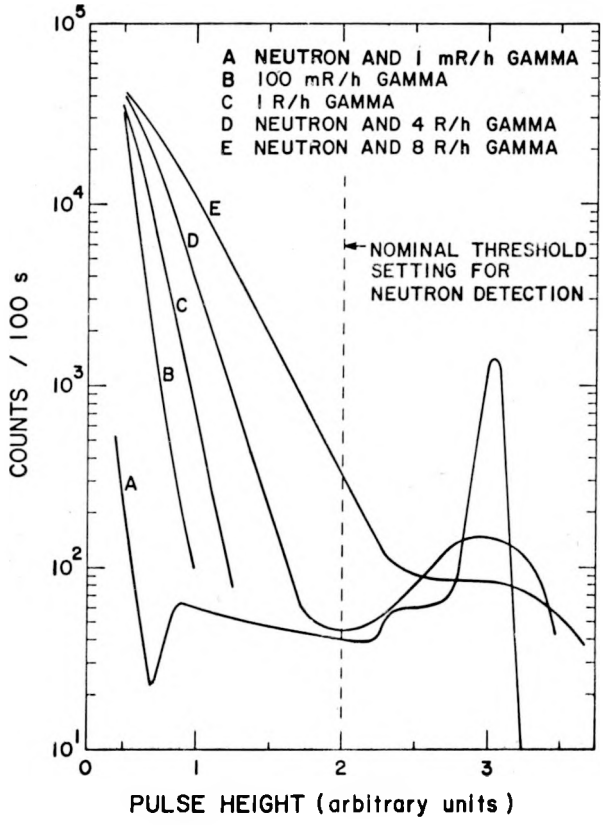

Fig. 2.
Gamma-ray pile-up effects for a ^{3}He proportional counter tube 2.54 cm in diameter and 50.8 cm in length.

To reduce the electronics we evaluated a hybrid circuit amplifier discriminator unit.* The units are produced in a 16-pin IC package and thus could be mounted in the high-voltage distribution box to make a very compact system. However, the gain of these units requires that the tubes be operated 500 V higher than normal. At higher operating voltages, resolution is lost and the maximum radiation limit is reduced by a factor of 5. Moreover, a higher voltage is more troublesome in humid climates. Therefore, we decided to reduce the electronics by grouping tubes and increasing the shielding. For the test setup nine tubes will be operated in parallel and only six sets of detector electronics will be used. With nine ^{3}He tubes for each set of electronics the maximum radiation dose should not exceed 100 mR/h, subsequently requiring the initial level of radiation to be attenuated by a factor of 1000.

The gamma-ray attenuation can be calculated from the fission product energy spectrum[9] shown in Fig. 3 and the mass absorption coefficients with dose build-up factors.[10] Figure 4 shows the gamma-ray dose attenuation as a function of lead-shielding thickness. It also shows the geometric effect of moving the detectors farther away from the barrel with increasing lead thickness. To achieve a factor of 1000 attenuation a 15-cm-thick lead shield is required.

A barrel surrounded on three sides by a 15-cm-thick lead shield (see Fig. 1) requires approximately 4.6 Mg (about 5 tons) of lead. Neutron transport codes indicate that neutron detection is not appreciably affected by the lead. However, background neutrons are produced by cosmic-ray interactions in the lead. For a passive coincidence counter, 4.6 Mg of lead result in a background coincidence rate corresponding to slightly over 100 g of plutonium (6% ^{240}Pu, measured at 2.2 km altitude); see Ref. 3, p. 18. For high-burnup reprocessed plutonium (about 20% ^{240}Pu) the corresponding background coincidence rate measured at sea level is an order of magnitude less.

The feasibility of suppressing cosmic-ray-induced neutrons was experimentally evaluated. The approach was to count the neutrons which immediately follow a detected cosmic ray and compare this rate to the overall rate attributed to the cosmic interactions in lead. The measurement was made by placing an 11.9-kg lead cube in a neutron well coincidence counter. Cosmic rays were detected by either a plastic Cerenkov detector* or a plastic scintillator** of the same size placed directly over the cube. The electronics were designed to count single and multiple neutron events and to simultaneously record those events which occurred within 100 μs following the detection of a cosmic ray. A background subtraction was made by counting without the lead in the neutron coincidence counter. The efficiency was defined as the probability of detecting the cosmic ray that initiated the neutron production in the lead. Results indicate the Cerenkov plastic had

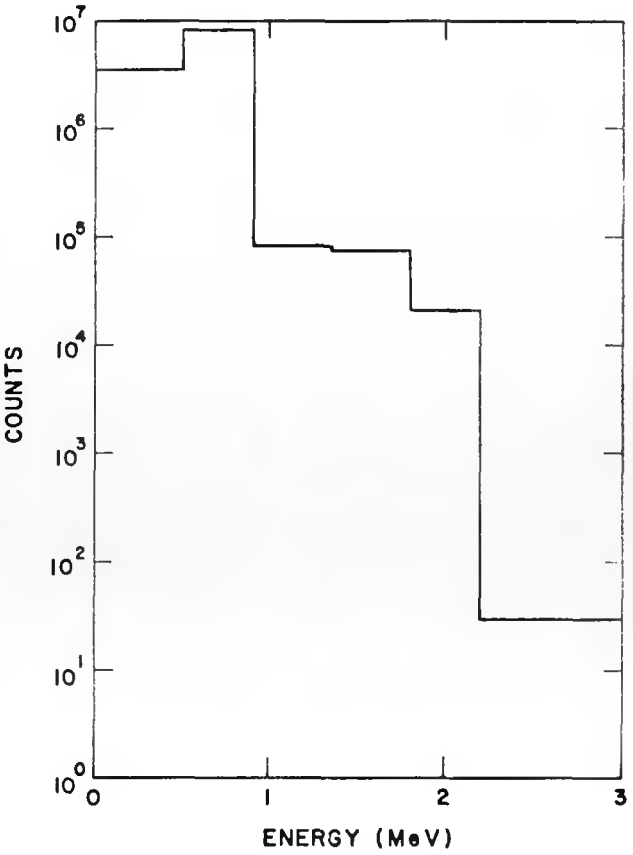

Fig. 3.
Approximated gamma-ray spectrum for mixed fission products.

Manufactured by LeCroy Research Systems, Model LD604L.

Manufactured by Nuclear Enterprises, Inc., material Pilot 425.
**ibid., material Pilot F.*

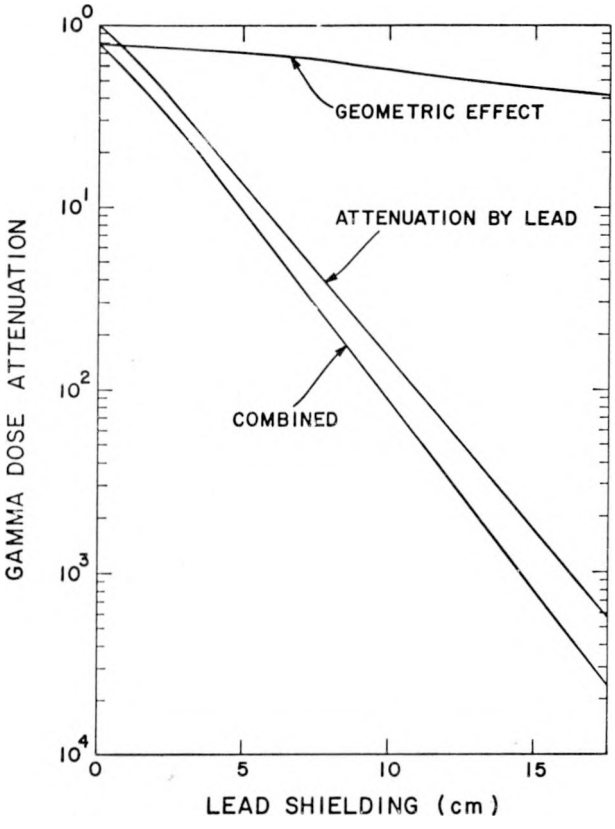

Fig. 4.
Attenuation of the gamma-ray dose for 55-gal barrel assay system.

an efficiency of 10.0 ± 1.5% for single events and 10.9 ± 2.1% for multiple events; the scintillation plastic had efficiencies of 61.5 ± 3.7% and 65.9 ± 2.7% for single and multiple events, respectively. We conclude that either the Cerenkov plastic has an intrinsically low efficiency or that a large fraction of the neutron-producing cosmics are low energy (nonrelativistic) and do not trigger the Cerenkov plastic. If the latter is true, then concrete surrounding the measuring area may provide significant shielding from cosmic rays. In either case, the efficiency of the Cerenkov plastic is too low to be useful. On the other hand, for a piece of scintillator plastic covering a barrel counter (1.6 by 1.6 m) the false alarm rate would produce essentially a 100% deadtime. Thus, neither plastic will be employed in the test setup shown in Fig. 1.

3. Neutron Transport Calculations (D. A. Close and T. W. Crane)

Monte Carlo calculations have been performed to determine the optimum amount of polyethylene moderator for the ^{3}He tubes. The efficiency and die-away time were calculated for various polyethylene thicknesses. The same thickness was assumed in front of and behind the tubes and a 5-cm spacing between centers was assumed for the tubes which are 2.54 cm in diameter. Calculated efficiencies are shown in Fig. 5 and neutron die-away times are shown in Fig. 6. The results are for carbon matrixes (ρ = 1 g/cc and ρ = 2 g/cc in 55-gal barrels). We also studied the effect of a 0.76-mm- (0.030-in.-) thick cadmium sheet placed between the lead and barrel. With the cadmium in the counter the system shows a maximum efficiency at 2.54-cm-polyethylene thickness, independent of matrix density; the die-away time increases monotonically with polyethylene thickness.

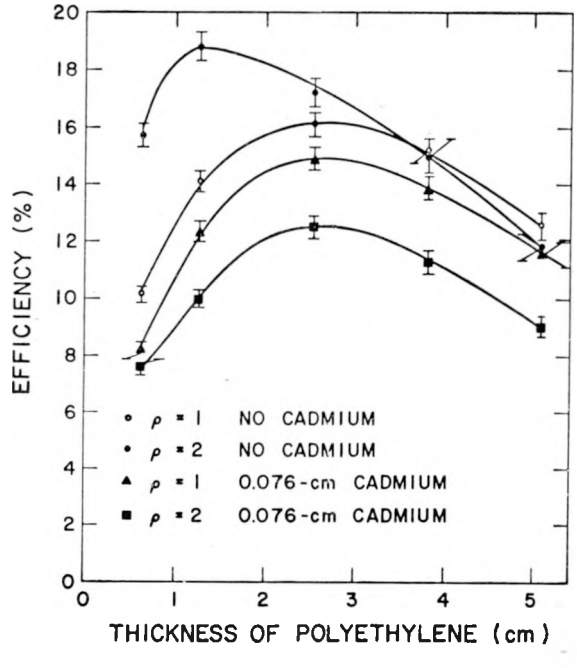

Fig. 5.
Neutron detection efficiency as a function of moderator wall thickness for a 55-gal barrel assay system.

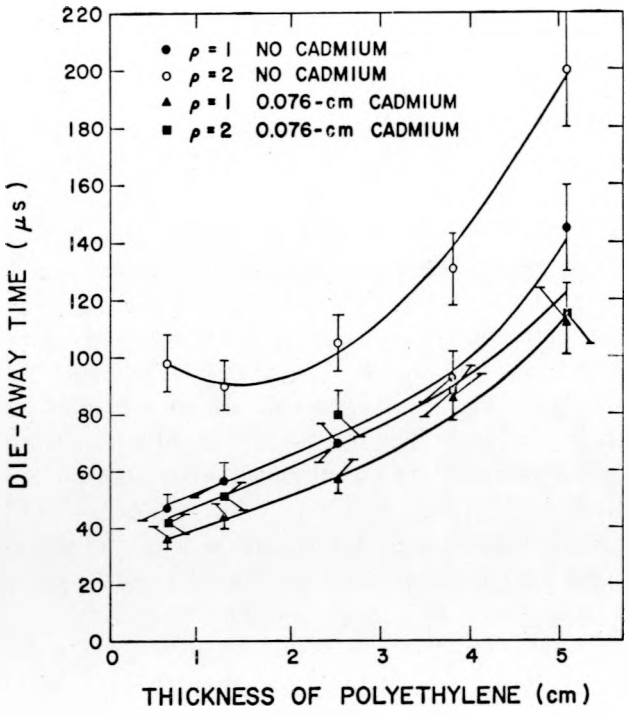

Fig. 6.
Counter neutron die-away time as a function of moderator wall thickness for a 55-gal barrel assay system. The curves serve only to guide the eye.

4. Germanium Detectors for Assay at 10 nCi/g (T. W. Crane)

The sensitivity and accuracy of an intrinsic germanium detector (1000 mm² in area by 12 mm thick) was evaluated for measuring TRU contamination in combustible waste at the 10 nCi/g fiducial. Two 57-ℓ (2 cubic foot) boxes were prepared by C. Nordeen and C. McCullough of Group CMB-11. The first box contained 16.8 mg of plutonium and the second 1.1 mg (94% ^{239}Pu, 6% ^{240}Pu). The plutonium content was estimated by two techniques: (a) comparison with the count rate of an 88-μg plutonium disc with corrections for geometric effects, background, ^{241}Am content, and attenuation within the box, and (b) we used the 16.8-mg box as a standard and obtained the ratio of the counting rates after corrections for background and ^{241}Am content. The L x-ray groups at 13.6, 17.3, and 20.5 keV had systematic errors of up to a factor of 4 for both boxes by the first method, and a consistent error of a factor of 2 by the second method. Assays using the ^{239}Pu gamma rays at 38.7, 51.6, and 129.3 keV had ±30% systematic errors for the 1.1-mg plutonium box using either technique; the 16.8-mg plutonium box had less than ±10% systematic errors for the gamma-ray analysis using the first method.

The box counter currently in use at the Group CMB-11 counting room employs an NaI detector 127 mm in diameter by 51 mm thick for assaying combustible waste.[11] Comparison of the detection sensitivity (3σ statistical) for the germanium detector (10 cm²) and the NaI detector (126 cm²) shows that the NaI detector is considerably more sensitive at the 10 nCi/g level (see Table IV). However, adequate sensitivity can be obtained with the germanium detector using the L x-rays and a 100-s counting time.

C. Extending the Versatility of the Random Driver (T. R. Canada, T. L. Atwell, D. A. Close, L. R. Cowder, N. Ensslin, and H. R. Baxman*)

In-plant applications have shown the Random Driver to be an accurate (1%) assay device with standards that are close replicas of the samples to be assayed.[18] However, some in-plant applications require the measurement of a wide variety of samples with a range of chemical compositions and properties for which it is impossible to produce a complete set of standards. One such plant is the uranium recovery facility at LASL.

The studies reported here were conducted using the Random Driver Mod V, which is a part of Group CMB-8's material balance system (Ref. 14, p. 4), with a view to extending its versatility and accuracy. The Mod V version is the same as the Mod IV version (described in Ref. 15, pp. 5-8) except that the Mod V was built with steel reflectors instead of nickel and contains a digital readout load cell.

1. Matrix Density Dependence

The materials routinely assayed vary in matrix densities, ρ_m, from approximately 0.5 g/cm³ to approximately 2.0 g/cm³. The matrix materials will down-scatter the average energy of both the Am-Li interrogation neutrons (the incident channel) and

*Group CMB-8.

TABLE IV

PLUTONIUM AND ^{241}Am DETECTABILITY LIMITS FOR A 1000-s COUNT

Photon Energy Region (keV)	Isotope	Detectability[a] (nCi/g)	
		Germanium[b]	NaI[c]
13.6, 17.3, 20.5[d]	Plutonium[e]	1.1	0.04
59.5	^{241}Am	0.016	0.0027
38.7, 51.6, 129.3	^{239}Pu	19	—
129.3	^{239}Pu	—	11

[a]Detectability limit at 3σ level, 57-ℓ box, 4 kg.
[b]Detector placed 40 cm from face of box.
[c]See Ref. 11, p. 8 and Ref. 12, p. 16.
[d]L x-rays with the ^{241}Am contribution removed.
[e]Plutonium with 94% ^{239}Pu and 6% ^{240}Pu.

the fission neutrons (the exit channel), by an amount proportional to ρ_m. A reduction of the incident neutron average energy will increase the fission rate per gram of ^{235}U. However, this will be corrected, to first order, by the ^{3}He flux monitor. The exit channel, on the other hand, will be scattered down to a region of lower detector efficiency (Ref. 16, p. 16), resulting in an overall reduction in the measured response per unit mass of ^{235}U.

This is demonstrated in Fig. 7a where the response is plotted vs the known mass of uranium M_U for three sets of standards which vary in ρ_m ($0.9 \lesssim \rho_m \lesssim 1.8$). A single calibration curve is clearly inadequate. Figure 7b shows the same data plotted as $R(\rho_m) = R/(1 - 9.3 \times 10^{-2}\ \rho_m)$ vs M_U and a linear least squares fit to the data (the solid line). The matrix correction thus allows a single set of standards to be used to calibrate the Random Driver for a wide range of samples with varying matrix densities. Note that the response is reasonably linear over the range of M_U studied (250 g $\leq M_U \leq$ 1600 g).

2. The ^{3}He Flux Ratio Correction Term

The response per unit mass of uranium, R/M, has been measured as a function of the ^{3}He tube flux ratio F for two masses of uranium, 0.5 and 4 kg. F was varied by wrapping the cans in various thicknesses of polyethylene. The results are shown in Fig. 8a.

An earlier estimate of the flux-correction term K had the form (Ref. 17, pp. 3-11)

$$K = 1 + 0.5(F - 1) .$$

This function does not depend on the mass of uranium present in the sample. Such a dependence would be expected because a component of the interrogating flux is being thermalized at the outer circumference of the sample and the fraction of the total uranium that sees this thermal component will depend on the density of uranium present. This dependence is reflected in the steeper slope of the line drawn through the 0.5-kg data.

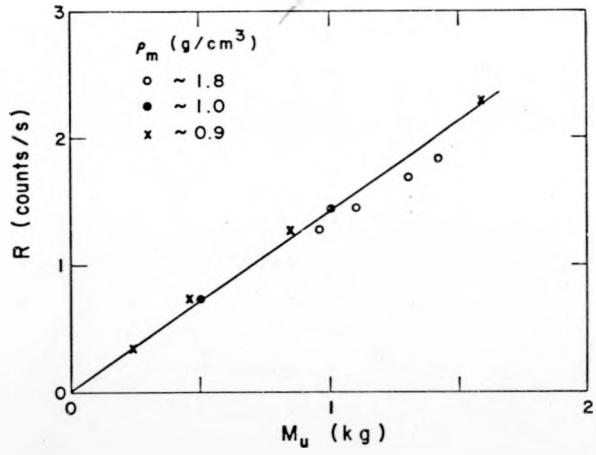

(a)

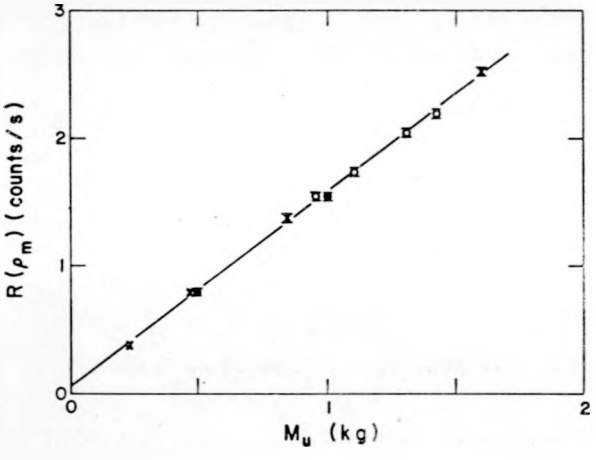

(b)

Fig. 7.
Measured Random Driver response vs mass of uranium for three sets of standards (a) before and (b) after the matrix density correction. The solid line in (b) is a linear least squares fit to the data.

Moreover, when small masses of uranium are being assayed ($\lesssim$100 g), it is desirable to increase the response per unit mass by acutely thermalizing the system, i.e., F $\geq$ 10. Preliminary data indicate that in such cases the earlier expression for K is much too small (Ref. 17, pp. 3-11).

On the basis of these observations, a new expression for K has been adopted,

$$K = 1 + x + \frac{x^2}{2}$$

where $x = (F - 1)\delta$ and $\delta = 0.33(1 - R \times 10^{-2})$; R is the uncorrected total neutron response. A plot of the flux-corrected response per unit mass, $R_c/M = (R/K)/M$ vs F is shown in Fig. 8b. These data show that this expression for K is adequate when F $\lesssim$ 2. Data are presently being collected for the F > 2 case.

Although it is expected that expressions for matrix density and ^{3}He flux ratio corrections will be similar for most Random Driver instruments, the absolute values of the parameters may vary, depending on the general type of material being assayed and the specific Random Driver design.

D. Ash-Leach Solution Assay Instrument (J. L. Parker, R. S. Marshall, R. Siebelist, and L. G. Speir)

The data acquisition and analysis system for the Solution Assay Instrument (SAI) consists of a high-resolution Ge(Li) detector, high-quality spectroscopy amplifier, pile-up rejector, digital stabilizer, and a Northern Scientific TN-1700 computer-based multichannel analyzer system. Analysis codes for the TN-1700 system are written in the interactive BASIC language. The system terminal is a General Electric TermiNet 30 with dual magnetic cassette accessory for code and data storage. In the near future the TN-1700 will be interfaced directly to a central computer which will receive results from several assay systems.

The volume of solution in the measurement bottles has been changed from 30 to 25 mℓ to reduce spillage. The sample bottles are right circular cylinders specially fabricated to tight dimensional tolerances. The sample within the bottle occupies a volume 3.57 cm in diameter by 2.5 cm deep, with a cross-sectional area of 10 cm^2. A Ge(Li) detector views the samples from the bottom at a distance of about 4.3 cm.

An extensive calibration- and performance-checking program is nearly complete. Analysis codes have been written and the system will go into routine

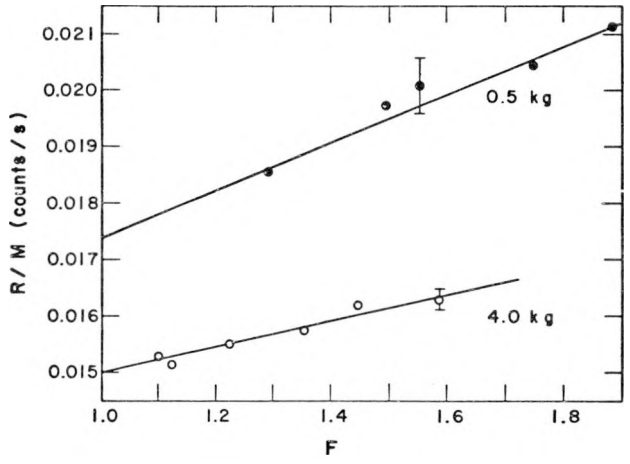

(a)

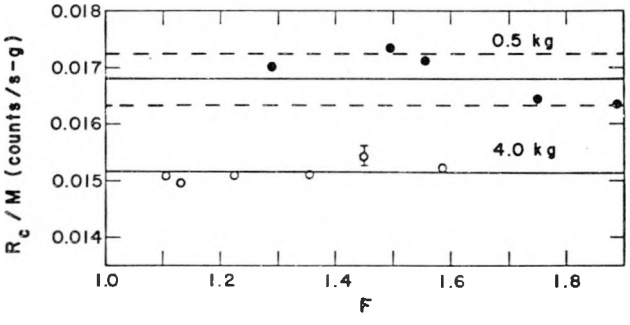

(b)

Fig. 8.
Measured response per gram of uranium vs the ^{3}He flux ratio F (lines are drawn through the data) and (b) flux-corrected response per gram of uranium vs F for two masses of uranium. Solid lines denote the average R_c/M. Dashed lines about the 0.5-kg average indicate the 1σ limits on the data.

use at the beginning of October. Accuracy information will be reported when the comparison study with Group CMB-1 is complete (see Part 2, Sec. II-A-4). However, it is now apparent what precisions are attainable. For example, a half-hour analysis will give ^{239}Pu determinations with precisions of ≤1% at the 1σ level for solutions with concentrations ≥1.0 mg of plutonium/mℓ and precisions of about 0.5% at the 1σ level for concentrations ≥5.0 mg of plutonium/mℓ.

SAI installation and checkout (previously described in Ref. 14, p. 8) is essentially complete. A cutaway view of the arrangement of the detector and sample holder assembly relative to the glovebox is shown in Fig. 9. The sample-holder assembly holds the sample bottle in a geometrically reproducible position, provides shielding of the Ge(Li) detector from extraneous plutonium above the detector, and contains the transmission source which is used in making corrections for the self-attenuation of the samples. Study has shown that for this application (solutions ≤10 g of plutonium/ℓ concentration) a plutonium transmission source is advantageous; accordingly, it consists of a 20-g nickel-plated plutonium disc 2.5 cm in diameter. In the current configuration, the 5-cm-thick tungsten shutter which is used to "turn off" the transmission source is manually operated.

As shown in Fig. 9, the Ge(Li) detector is mounted with its lead shielding under the glovebox. (The detector is roughly 11% efficient in the usual definition with approximately 1.7-keV FWHM resolution

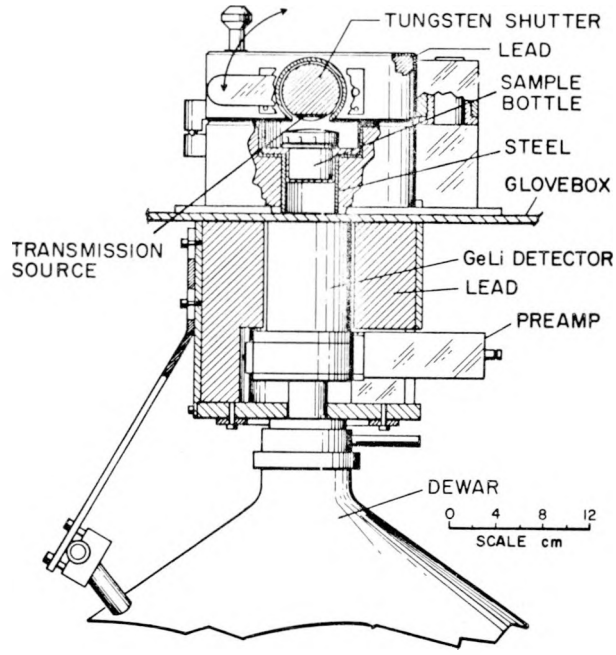

Fig. 9.
Plutonium solution measurement system.

at 1332 keV.) The bottom of the glovebox (approximately 2.5 mm of stainless steel) and 0.5 mm of cadmium provide adequate filtering of the intense low-energy radiation from the solutions. A small ^{109}Cd source is fastened directly to the face of the detector to act as a reference source for correction of rate-related counting losses and to provide a low-energy stabilization peak. This ^{109}Cd source provides a rate of about 10^3 s^{-1} in the full energy peak (88.0 keV) which is adequate for this application.

II. INSTRUMENT DEVELOPMENT AND MEASUREMENT CONTROLS

A. Portable High-Level Neutron Coincidence Counter (H. O. Menlove, N. Ensslin, M. L. Evans, and J. E. Swansen)

Design and fabrication of the detector portion of the portable thermal-neutron coincidence counter has been completed for use by the International Atomic Energy Agency (IAEA). This detector has been optimized for assay of high-content plutonium samples and for portability by inspectors. The coincidence detector (see Ref. 16, Fig. 6) can be used as a well detector or a flat slab-type detector depending on the application.

The coincidence detector is currently being tested for efficiency and neutron die-away time. The preliminary results of the measurements indicate an efficiency of 6.3 ± 0.5% and a die-away time of 18.7 ± 0.5 μs which are optimum for measuring samples in the mass range of 500-2000 g of PuO_2.

Three different electronic coincidence circuits are being evaluated for use with this portable counter. The three circuits are the variable delay circuit developed by Birkhoff et al. at EURATOM,[18,19] the shift register circuit,[20] and a new updating one-shot circuit. Initially the variable delay circuit looked most promising because of its simplicity. However, a close evaluation of its use showed that it gave fictitiously high plutonium assays when the room background changed during a counting period. This problem can be predicted from the data reduction equations and can be corrected by real-time data reduction during the data collection. However, the simplicity of the circuit is then lost.

For IAEA inspection applications, the above problem with the variable delay circuit is especially worrisome because there is no control over room background, thus it was eliminated as prime candidate for the present application. The remaining two coincidence circuits are presently being intercompared for use with the IAEA portable counter.

B. Neutron Correlation Studies (N. Ensslin, J. E. Swansen, and H. O. Menlove)

A study is in progress of three electronic circuits for use with thermal-neutron coincidence counters. The deadtime corrections and statistical errors associated with each circuit are being calculated, and the results compared with experiment. Through this work we seek to understand the limitations and advantages of each circuit in the assay of spontaneous neutron emitters.

We have continued the study of the variable deadtime counter (VDC) described in Ref. 14, p. 8 and Ref. 16, p. 13. The following formulas have been found to yield an assay that is independent of accidental background rate (within statistical error). The formulas have been tested under a wide variety of conditions for accidental rates up to 80 kc, and involve no free parameters.

$$R = \frac{\left[\frac{s_1}{1-s_1\tau_1} - \frac{s_2}{1-s_2\tau_2}\right](1+A\tau_d)}{\left[\frac{\exp(-\tau_1/\tau_d)}{1+A\tau_1} - \frac{\exp(-\tau_2/\tau_d)}{1+A\tau_2}\right]} \qquad (1)$$

$$A = \frac{s_1}{1-s_1\tau_1} - \frac{R}{1+A\tau_d}\left[A\tau_d + \frac{\exp(-\tau_1/\tau_d)}{1+A\tau_1}\right] \qquad (2)$$

$$\frac{\sigma_R}{R} \approx \frac{\frac{1}{T}\left[\frac{s_1 T}{(1-s_1\tau_1)^2} + \frac{s_2 T}{(1-s_2\tau_2)^2} - \frac{2s_2 T}{(1-s_1\tau_1)(1-s_2\tau_2)}\right]^{1/2}}{\left[\frac{s_1}{1-s_1\tau_1} - \frac{s_2}{1-s_2\tau_2}\right]} \qquad (3)$$

R = real coincidence rate, proportional to the amount of fissionable material,

A = accidental coincidence rate,

τ_1 = gate length of first nonupdating one-shot,

τ_2 = gate length of second nonupdating one-shot,

s_1 = count rate in scaler attached to first one-shot,

s_2 = count rate in scaler attached to second one-shot,

τ_d = die-away time of thermal-neutron coincidence counter,

T = length of run in seconds.

Equations 1 and 2 are coupled equations that are most easily solved by iteration. Very few iterations are required, because R ≪ A for those cases where the equations represent a substantial correction to the simple formula

$$R = \frac{\left[\frac{s_1}{1-s_1\tau_1} - \frac{s_2}{1-s_2\tau_2}\right]}{\exp(-\tau_1/\tau_d) - \exp(-\tau_2/\tau_d)} \quad . \qquad (4)$$

Equations 1 and 2 have been derived in part from first principles and in part from measurements of the distribution of time intervals between real and accidental events. A formal proof is still lacking, and the equations can be considered semiempirical. Up to the present time they have given correct results for all values of R, A, τ_1, τ_2, and τ_d that have been tried.

Equation 3 is based on the experimental result that the relative statistical error in R is essentially the same as the relative error derived from the simple formula (Eq. 4) alone. The first two terms within the radical in Eq. 3 are derived from the fact that, for nonupdating one-shots, the fractional standard deviation in the count rate is just $1/\sqrt{s_1}$ or $1/\sqrt{s_2}$, respectively.[21] The third term within the radical represents a reasonable guess about the degree of correlation between the rates s_1 and s_2, but has not been proved.

Figure 10 illustrates the assay of 13 g of ^{240}Pu in the presence of an accidental background. A neutron coincidence counter with an efficiency of 6% and a thermal-neutron die-away time of 19 μs was used. The VDC one-shots had lengths of 4.025 and 32.025 μs. The shift register was operated with a gate length of 32.5 μs and a predelay of 4 μs. The LASL VDC circuit consists of two one-shots whose lengths are precisely determined by counting a 20-MHz crystal-controlled oscillator. This feature eliminates the need for calibration with an accidental source as well as the need for arbitrary adjustments to τ_1 and τ_2 in Eqs. 1 and 2.

The data in Fig. 10 consist of five 1000-s runs at each value of the accidental rate. Each plotted point is the mean of the five points, and the error bars are the observed scatter of the five points, divided by $\sqrt{5}$. The assay (R = 0.04 kc) is independent of accidental rate within statistical errors which are well represented by the calculated error, Eq. 3. At the

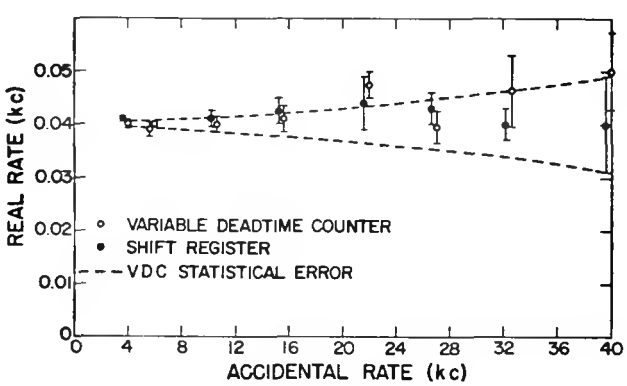

Fig. 10.
Assay of 13 g of ^{240}Pu as a function of different accidental backgrounds due to (α,n) reactions in the sample and a nearby Am-Li source.

first data point the ratio of accidental to real coincidences is 100 to 1. This ratio is due to the multiplicity of ^{240}Pu, the efficiency of the counter, and the occurrence of (α,n) reactions in the PuO_2, and is a typical ratio for any size PuO_2 sample in the present counter. Under these conditions the assay is accurate to ≤5%. The last data point has a ratio of accidentals to reals of 1000 to 1, and represents the limit of the VDC for any practical counting times. This ratio was obtained here by introducing a strong Am-Li(α,n) source, and would probably never occur in actual assay conditions. If a 1- or 2-kg PuO_2 sample produced an accidental rate near 40 kc, the real rate would be near 0.4 rather than 0.04 kc.

The second circuit under study is the shift register.[20,22] Figure 10 compares data taken concurrently with a shift register and a VDC to yield the somewhat surprising result that both circuits give the same assay and have comparable statistical errors. An analysis of the deadtimes present in the shift register is currently under way. At present we do not completely understand the corrections required at rates above 20 kc.

The third circuit under study consists of two updating one-shots of equal length, one being delayed with respect to the other, as illustrated in Fig. 11. This circuit is similar to an earlier circuit described by Strain and Omohundro[23] which employed nonupdating one-shots. The present version is conceptually easier to analyze and produces a circuit somewhat similar to the shift register in concept but easier to construct. A particularly promising version of this circuit under study lengthens the assay run to correspond to the true livetime. This circuit seems to require no further deadtime corrections except for those associated with the detector.

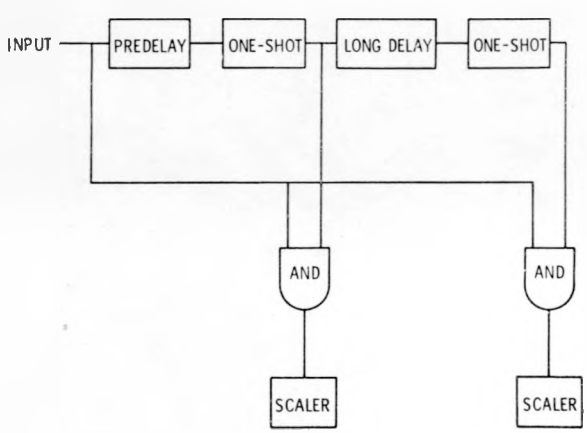

Fig. 11.
Updating (one-shot)-(delayed-one-shot) circuit. The two one-shots are of equal length.

Comparison of this circuit with the VDC and the shift register is not yet complete. It seems to be true, however, that the results of all three circuits can be properly corrected for deadtime effects to give the same assay up to at least 40 kc. If the lengths of the one-shots and coincidence intervals are comparable, all three circuits will also show the same statistical scatter in the data. This result is not yet completely understood.

One comparison of the three circuits that has been completed concerns the effect of a large change in the accidental background during the run. The results of such a change are tabulated in Table V. Run 1 represents the assay of an amount of fissionable material equivalent to 483 g of PuO_2 (18% ^{240}Pu) for 1000 s. During run 2 an additional background rate equivalent to the accidental coincidences from 800 g of PuO_2 was present inside the neutron coincidence counter. During run 3 this additional accidental material was introduced halfway through the run. The VDC circuit measures only the average rate during the run, and is completely vulnerable to such a change. The shift register and the updating one-shot circuits record real and accidental coincidence intervals on a real-time basis, and are insensitive to such changes, although corrections for amplifier and electronic deadtimes may be affected by a few percent. Thus the latter circuits seem to be more useful for general field applications.

C. Unirradiated Fuel Assembly Verification by Passive Neutron Counting (H. O. Menlove, M. deCarolis,* T. Dragnev,* and A. Keddar*)

For inspection and verification purposes, the IAEA recently pointed out[24] the need for a nondestructive assay (NDA) measurement of the ^{235}U enrichment in unirradiated boiling water reactor (BWR) and pressurized water reactor (PWR) fuel rod assemblies. The measurement technique should

Staff members of the Department of Safeguards and Inspection, IAEA Headquarters, Vienna.

TABLE V

INTERCOMPARISON OF THERMAL-NEUTRON COINCIDENCE CIRCUITS FOR VARIABLE BACKGROUND RATES[a]

Run	Average Total Rate (kc)	VDC Assay (g)	Shift Register Assay (g)	Updating Circuit Real-Time Assay (g)	Updating Circuit Livetime Assay (g)
1	1.6	456 ± 1	483 ± 3	472 ± 2	471 ± 3
2	12.0	446 ± 5	482 ± 10	477 ± 15	480 ± 4
3[b]	6.6	3 098 ± 3	483 ± 4	481 ± 7	479 ± 4

[a]The standard deviation was obtained by repeating each run three times.
[b]For run 3, the random background rate was changed by more than a factor of 10 during the measurement.

be suitable for field application by an inspector using portable equipment. The IAEA is evaluating several different NDA methods for this purpose including passive gamma-ray counting, passive neutron techniques, x-ray film exposure, and active neutron interrogation.

The present work evaluates passive neutron counting to determine the ^{235}U enrichment in a BWR assembly. The use of passive neutrons is very attractive for this application because they are fast (approximately 1-2 MeV) and thus able to penetrate from the interior of the fuel assembly as well as from protective containers. An unirradiateed assembly gives off neutrons from two sources. The dominant source,* unfortunately, is the spontaneous fission of ^{238}U which is of secondary interest and adds a background to the measurement. The neutron source of interest is the (α,n) yield of ^{234}U with oxygen because ^{234}U enrichment is roughly proportional to ^{235}U enrichment.

Table VI gives the masses and expected neutron yields from ^{238}U and ^{234}U for a section of a light water reactor (LWR) assembly containing 10 kg of UO_2.

The $^{238}UO_2$ also emits (α,n) neutrons with a yield of about 2-3% of the spontaneous fission yield. These (α,n) neutrons are neglected in the present discussions.

TABLE VI

PASSIVE NEUTRON YIELDS FROM 10 kg OF UO_2

Source	Percent Enrichment 1%	2%	3%
^{238}U (g)	8 727	8 638	8 550
^{235}U (g)	88.1	176	264
^{234}U[a] (g)	0.72	1.43	2.15
Spontaneous fission (n/s)	96	95	94
^{234}U (α,n) yield (n/s)[b]	10	20	30
Fraction of neutrons from ^{234}U	0.07	0.17	0.24

[a]Grams of ^{234}U were obtained from assumed wt% $^{235}U/^{234}U$ = 123.
[b]Neutron yield for $^{234}UO_2$ was taken as 14 n/s-g.

The ^{234}U mass was calculated from ^{235}U using a $^{235}U/^{234}U$ ratio of 123 which was obtained from mass spectroscopy data (Ref. 25, pp. 20-22) for low enrichment UO_2. For 2% enriched fuel about 80% of the neutron yield is from the spontaneous fission of ^{238}U. An assay device will sample 10-20% of the fuel length of a full assembly containing roughly 300 kg of UO_2. The mass of UO_2 contributing to the neutron yield would be 30-60 kg, and thus, the $^{234}U(\alpha,n)$ yield for 2% ^{235}U fuel would be approximately 100 n/s. A CH_2 moderated detector containing a single ring of ^3He tubes would have a counting efficiency of roughly 15% resulting in a net signal rate of approximately 15 counts/s.

For our investigation, a series of passive neutron measurements were performed using the IAEA's mockup BWR assembly, an 8- by 8-rod array containing BWR rods about 50 cm long. The assembly contains 64 rods which have three different enrichments: 1.40, 2.05, and 2.50% ^{235}U. The neutron yield from the assembly was measured using four ^3He detectors (2.5 cm in diameter by 20 cm long at 4 atm fill pressure) inserted into a polyethylene holder approximately 5 cm thick.

To measure the yield as a function of enrichment, 20 rods of each enrichment were placed in the assembly and the total neutron yield was measured. Figure 12 shows the results of the measurements as a function of ^{235}U enrichment. Each data point represents the average of three runs of 1000 s each. The extrapolation of the curve to zero ^{235}U gives the neutron contribution from ^{238}U, the room background having been previously subtracted from the data. For a ^{235}U enrichment of 2%, the $^{234}U(\alpha,n)$ fraction of the neutrons in Fig. 12 is 0.19, which is in good agreement with the calculated fraction of 0.17 given in Table VI.

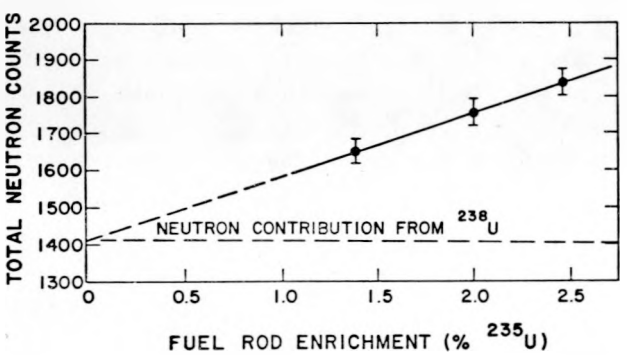

Fig. 12.
Passive neutron yield from the IAEA BWR fuel assembly mockup.

The key question in the application of this technique is how well the neutron yield predicts the ^{235}U enrichment. First one must assume that the ^{238}U spontaneous fission neutron contribution is known by weighing or gamma-ray techniques. Then the residual neutron yield can be related to the ^{234}U content by use of standard assemblies. However, the $^{235}U/^{234}U$ ratio has a scatter depending on the enrichment history. For example, mass spectrometer analysis (Ref. 25, pp. 20-22) of 16 UF_6 samples ranging in enrichment from 0.71 to 3.98% gave an average $^{235}U/^{234}U$ ratio of 123 ± 9 (1σ). This represents a 7% uncertainty in converting from the ^{234}U to the ^{235}U content. All of these samples were from the same gaseous diffusion plant. Samples from different diffusion plants or centrifuge enrichment plants would likely have a larger deviation in their $^{235}U/^{234}U$ ratios.

In summary, there are several problems with applying passive neutron counting to fuel assemblies to determine ^{235}U content.

(a) The ^{238}U content in the assembly must be determined independently.

(b) Normal variations in the $^{235}U/^{234}U$ ratio can be expected to be greater than ±7% (1σ) or greater than ±14% (95% confidence level).

(c) If the enrichment plant handles reactor returns, the neutron yield will increase because of the presence of ^{232}U.

(d) Room background neutrons from sources such as other fuel assemblies, radioactive neutron sources, or nuclear reactors are very difficult to shield against and can easily perturb the results. (Our investigation was performed at the Atominstitut der Oesterreichischen Hochschule. The first set of measurements was invalidated by the movement of a plutonium source in the room, the second set was lost because the reactor at the site operated at variable power levels, and the third set of measurements was lost because a Pu-Be neutron source was moved into an adjacent room.)

(e) A large volume, high-efficiency neutron detector would require a detector mass of about 30 kg and necessary shielding of about 80 kg, precluding its portability.

Because item b limits the ultimate accuracy of this passive neutron method, there is little motivation to achieve high precision in the counting statistics. That is, 600 counts results in a standard deviation of ±4%; this precision can be obtained with the present SNAP II counter (Ref. 14, pp. 5-7) in about 10 min. The SNAP II counter has the advantage of being small, portable, and relatively easy to shield from room neutrons.

In conclusion, passive neutron counting of LWR fuel assemblies should not be used for accurate loading determinations. However, the method is extremely simple with good penetration into the interior of the assembly. The method may prove useful for verifying that assemblies have not been altered in ^{235}U content from one inspection to the next.

D. Portable Neutron Assay for Light-Water Reactor Fuel Assemblies (J. D. Brandenberger, H. O. Menlove, E. Medina, and R. Siebelist)

The development of a portable NDA method for verification of LWR fuel assemblies needed by the IAEA for inspection purposes[24] has been completed to a useful state for BWR fuel assemblies which do not contain burnable poisons. This development was described in the previous status report (Ref. 16, p. 12). The assay system for the BWR 6-by-6 array gives a fairly flat response for all rod locations. It can detect the removal of any rod or the substitution of any four rods of 1.77% ^{235}U for rods of 2.34% ^{235}U.

Additional development has focused on improving the assay system for PWR fuel assemblies. This is a more difficult problem because (a) the fuel assemblies have configurations of larger arrays of fuel rods, and (b) the assemblies vary in configuration from different manufacturers and even from the same manufacturer. Fuel rod arrays differ in the number of pins and may or may not have locations for control rods.

Development work has been done using a modification of the BWR assay system and a partially filled 15-by-15 United Nuclear fuel assembly shown in Fig. 13. This assay system has been used with a ^{241}Am-Li neutron source with a source strength of $4.3 \times 10^5\ s^{-1}$. The hollow channels cut in the CH_2 moderator are to give a more uniform neutron flux distribution across the PWR assembly. Figure 13 shows regions 1-12 into which the system has been divided for test purposes. For testing, fuel

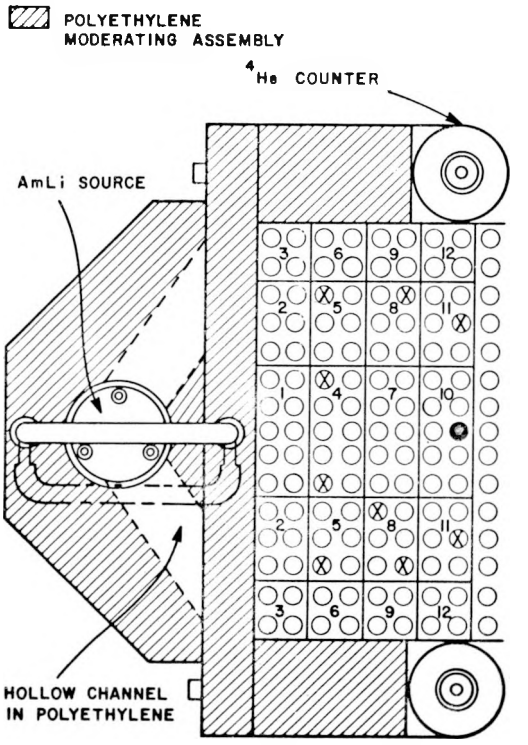

Fig. 13.
PWR fuel assembly assay system. The small circles represent individual fuel rods in part of a 15- by 15-rod assembly. The circles with an X are possible locations for control rods.

rods in one region at a time are replaced by steel rods. The assay system is sensitive to regions near the edge, i.e., regions 1-3, 6, 9, and 12. Typically in these regions, a single rod replaced by a steel rod is at the threshold of sensitivity (1σ count rate decrease) of the assay system. Because this partially filled fuel assembly contains 135 rods, the assay system has a sensitivity of about 1% for missing ^{235}U in the edge regions. For inner regions 4, 5, 7, 8, 10, and 11, the assay system is less effective because the thermalized neutrons from the ^{241}Am-Li source have difficulty in penetrating into the interior regions. From the inspector's point of view, these interior regions are the most important for the very reason that they are the most difficult to measure. Table VII gives typical results in the decrease in counts/rod-1000 s and the number of fuel rods replaced by steel rods required for detection. Similar results were obtained for the fuel assembly with the control rod positions left vacant and for a 13-by-13

TABLE VII

SENSITIVITY TEST RESULTS OF PORTABLE PWR ASSAY SYSTEM FOR PARTIALLY FILLED 15- BY 15-ROD FUEL ASSEMBLY

		Sensitivity at the 2σ Level	
Region[a]	Decrease in Counts/Rod-1000 s[b]	Rods Exchanged for Detection	Percent of Rods Exchanged
1	271	2	2
2	255	2	2
3	277	2	2
4	122	4	3
5	145	3	2
6	193	3	2
7	75	6	5
8	90	5	4
9	190	3	2
10	69	7	5
11	75	6	5
12	150	3	2

[a]Region in which steel rods have been substituted for fuel rods.
[b]The standard deviation of the measurements is 220 to 260 counts/rod-1000 s.

array, respectively. In examining this table it should be noted, for example, that five rods represent only 4% of the total in regions 1-12 and 2.5% of an entire 15-by-15 array. Because the present PWR mockup contains only 135 rods (15-by-9 array), the full effect of thermal-neutron absorption has not been measured. An additional group of PWR rods has been obtained to complete the 15-by-15 array to better determine the neutron absorption in the interior section of the mockup PWR assembly.

Further efforts are being made to improve the sensitivity of the PWR assay unit. Whereas the source-moderator geometry is considered near optimum for a unit which must be highly portable, the ^{4}He detectors are only about 0.5% efficient. More efficient scintillators to be used in a gamma-ray rejection mode have been ordered for testing with the system. This has the possibility of more than doubling the sensitivity of the instrument. Because of the vast range of the configurations of PWR fuel assemblies, final test of our PWR assay system will have to be conducted in the field where the various configurations are available.

E. Experimental Photoneutron Assay of Intermediate-Size Samples (M. S. Krick and H. O. Menlove)

Photoneutron systems have previously been constructed for the assay of fuel rods and small samples (Ref. 6, p. 16), and spent Rover fuel elements (Ref. 12, p. 8). Further experiments have been performed with a ^{124}Sb-Be assembly to study the sensitivity, linearity, and spatial dependence of assays of intermediate-size samples. Photoneutron interrogation techniques are under consideration for assaying full fast flux test facility (FFTF) fuel assemblies.

The experimental arrangement, shown in Fig. 14, was set up in a Group R-1 hot cell. The 10- by 20.5-cm sample-irradiation cell contains a ^{124}Sb-Be neutron source and a sample holder. The ^{124}Sb-Be neutron source consists of an 8-mm-diam by 8-cm-long ^{124}Sb gamma-ray source (about 2 Ci) in the center of a 7.5-cm-diam by 10-cm-high beryllium cylinder. The sample holder is a light-weight assembly made from thin aluminum sheet and has positions for up to 25 small samples. The irradiation cell is

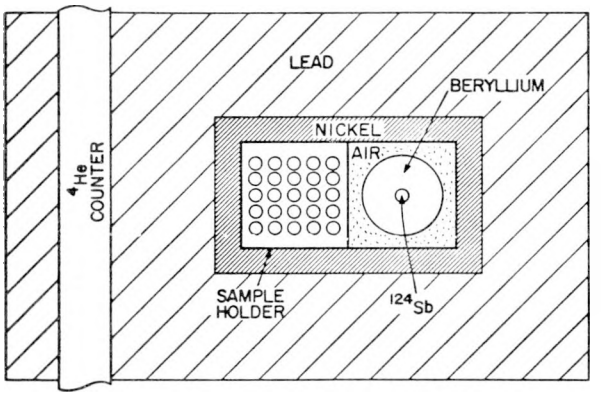

Fig. 14.
Experimental photoneutron assay system, top view.

	8.2	-1.4	-0.4	-1.5	0.2
	13.8	2.5	0.1	-0.6	6.2
^{4}He ←	15.8	2.8	0	2.2	9.2 → ^{124}Sb
	12.4	3.6	-0.3	-1.6	5.9
	13.4	0.7	-2.9	-4.1	4.9

Fig. 15.
Spatial dependence of the photoneutron assay system response. The blocks represent the 25 sample positions; the numbers in them are percent deviations relative to the central position. The ^{124}Sb source is to the right and the ^{4}He detector is to the left.

surrounded on the sides and bottom with 2.5 cm of nickel for neutron reflection and 10 cm of lead for gamma-ray shielding. To simplify insertion of the samples and the ^{124}Sb source, the top of the assembly is not covered.

The fast-neutron detector consists of a single, 18-atm, 5-cm-diam, 50-cm-long, ^{4}He proportional counter placed outside the irradiation cell opposite the ^{124}Sb-Be source. The counter is operated at 1800 V with bipolar, resistor-capacitor (RC) pulse shaping and 0.5-μs time constants. An additional 5 cm of lead is placed behind the counter for neutron reflection and, hence, improved detection efficiency.

The spatial dependence of the system's response was studied by counting a 9.3-g ^{235}U sample (93% enriched UO_2) for 1000 s in each of the 25 sample-holder positions. The result of these measurements is shown in Fig. 15, where the number shown for each sample location indicates the percent difference in response relative to the central position. The diagram is a top view of the system with the ^{124}Sb source on the right. The standard deviation for each 1000-s measurement due to counting statistics only is about 1.8%. Relative to the central position, the system response is high for positions on the left side of the diagram (where the sample is close to the detector) and on the right side (where the sample is close to the interrogating neutron source). However, the response is remarkably uniform over the central 6- by 6-cm region; the average deviation measured for the nine central positions is only 1.1%.

The linearity of response vs sample mass was studied for the central position of the sample holder by counting eight samples, containing 0.93 to 9.3 g of ^{235}U, for 1000 s each. No statistically significant deviation from linearity was observed. A similar linearity study was performed over the nine central sample positions by counting from one to nine samples with masses ranging from 3.7 to 9.3 g of ^{235}U per sample. With all nine samples inserted the total ^{235}U mass was 56.8 g. The result is shown in Fig. 16, where the straight line is a visual fit to the data and where the error bars indicate one standard deviation due to counting statistics only. It is not clear whether the low responses for total masses above 50 g of ^{235}U are due to counting statistics, positional dependences, or sample absorption effects; Monte Carlo calculations and measurements with larger sample masses are planned.

Figure 17 shows a pulse-height distribution taken with the ^{4}He proportional counter for 1000 s with 58.6 g of ^{235}U in the central nine sample-holder positions. A 1000-s background spectrum is also shown for comparison. The high-energy background is due primarily to ^{252}Cf sources stored in the hot cell where the photoneutron measurements were performed.

The sensitivity of this experimental system is 0.2 counts/s-g-Ci when ^{235}U samples and ^{124}Sb sources are used. The sensitivity could easily be increased by more than an order of magnitude with the use of

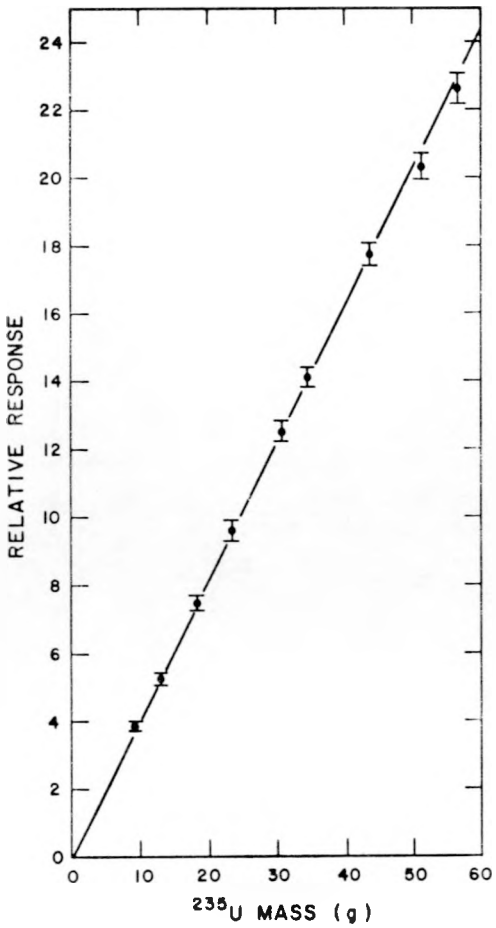

Fig. 16.
Photoneutron assay system response vs ^{235}U mass for one to nine samples in the central nine sample positions.

multiple ^{4}He counters. As an illustration, if the sensitivity is increased to 2 counts/s-g-Ci and if a 10-Ci ^{124}Sb source is used, then a 100-g sample of ^{235}U can be measured to a statistical precision of 0.5% (1σ) in 20 s.

F. Gamma-Ray Energies for Plutonium Absorptimetry (D. G. Langner and T. R. Canada)

Terrey and Dixon[26] have employed an absorptimetry technique to determine uranium densities ρ_u in solutions where $250 < \rho_u < 350$ g/ℓ. With this technique, the transmission T of the ^{241}Am, 60-keV gamma ray is measured through a solution sample. The transmitted gamma rays are detected in an

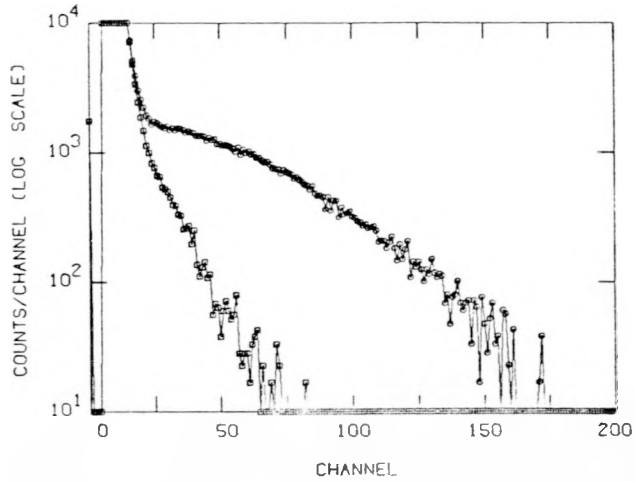

Fig. 17.
Pulse-height distributions taken from the ^{4}He counter in the photoneutron assay system with and without a 57-g ^{235}U sample.

approximate 4π geometry in order to reduce the effects of variations in the low Z matrix constituents. The uranium density is then given by

$$\rho_u = -\frac{\ln T}{\mu_u x} - \left(\frac{\mu_m}{\mu_u}\right)\rho_m \qquad (5)$$

where x is the sample thickness, μ_u and μ_m are the photoelectric mass absorption coefficients for uranium and the matrix at 60 keV, and ρ_m is the matrix density. The system is calibrated with a set of standards for which ρ_m and μ_m are assumed the same as for the samples which are to be assayed.

This technique cannot be viewed as an effective safeguards procedure, in that the substitution of medium or high Z materials for uranium in the solution will not be detected. However, the question arises that, if the technique is to be used, is there a gamma-ray energy at which the measured special nuclear material (SNM) density is less sensitive to matrix contaminants?

For plutonium solutions, the ^{57}Co, 122-keV gamma ray appears to be preferable to the 60-keV gamma ray used in the uranium work. This energy is immediately above the plutonium K-absorption edge. From Eq. 5 the influence on the assay of a contaminant with a photoelectric mass absorption coefficient μ_c is proportional to the ratio μ_c/μ_{Pu}.

This ratio has been calculated as a function of atomic number Z for the two energies, 60 keV and 122.0 keV.[27] A plot of these ratios is shown in Fig. 18. The calculations indicate that, for matrix comtaminants with Z < 69, use of the 122.0-keV transmission source will result in smaller errors in the measured plutonium content. The cost of using this higher energy source is a 35% reduction in transmission sensitivity due to the decreased mass absorption coefficient of plutonium, and the necessity of replacing the ^{57}Co source periodically, due to its shorter half-life (272 days).

G. Gamma-Ray Densitometry

1. K-Absorption Edge Techniques (T. R. Canada, J. W. Tape, and E. R. Martin)

The segmented gamma scanner[28] (SGS) measures ^{239}Pu content in cans by means of a transmission-corrected count of the 413.7-keV ^{239}Pu gamma ray. In addition to the gamma ray at 400 keV, the transmission source ^{75}Se has gamma rays at 121.1 and 136.0 keV which straddle the plutonium K-absorption edge, and thus may be used to determine the total plutonium mass present within a sample. For a fixed segment width h_s the plutonium mass in a can with diameter d is given by

$$M_{Pu} = C \sum_n \ln(R_n)$$

where R_n is the ratio of the 136-keV transmission to that of the 121-keV transmission, for the nth segment and $C = -h_s \pi d / 4\Delta\mu$; $\Delta\mu$ is the difference in the plutonium mass absorption coefficients at 136 and 121 keV.

To demonstrate this technique two plutonium-ash can standards (d = 8.33 cm) were assayed with nominal segment widths of 1.27 cm (0.5 in.). The results are shown in Fig. 19 where $-\ln(R_n)$ is histogrammed as a function of height measured from the bottom of the can. The assay values, 21.4 and

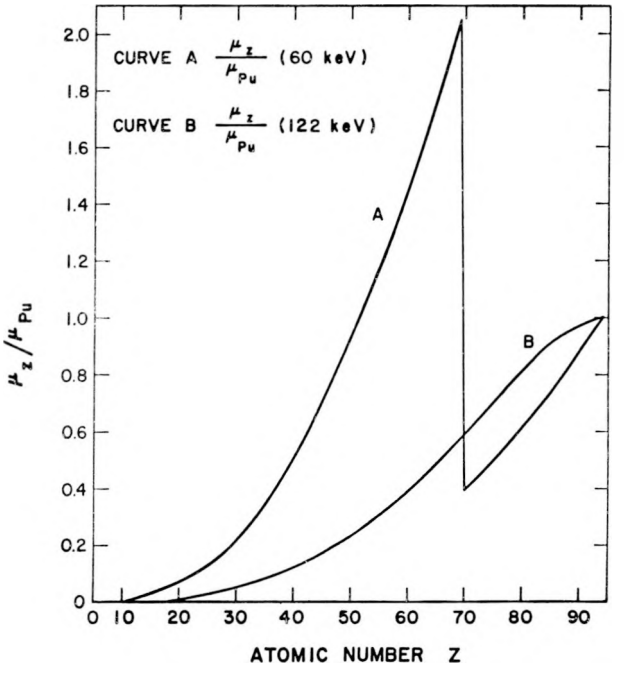

Fig. 18.
Ratio of the photoelectric mass absorption coefficient of an element of atomic number Z to that for plutonium at 60 and 122 keV.

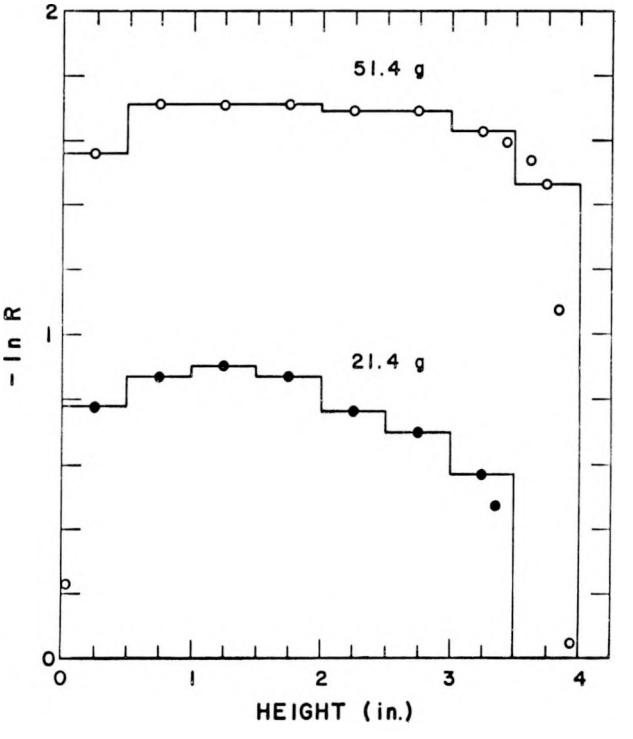

Fig. 19.
Negative logarithm of the measured ratio of the 136-keV to the 121-keV gamma-ray transmission R through two plutonium-ash cans as a function of height in the can.

51.4 g (± 2%), are in agreement with the nominal values of 21.97 and 51.4 g, respectively.

These data are available in the routine use of the SGS for the assay of plutonium and may be used as an independent, simultaneous measurement of plutonium mass or as a check on assumed ^{239}Pu enrichment.

The ^{75}Se single source measurement has a number of advantages. It does have a major disadvantage, in that the 136-keV gamma ray is approximately 15 keV above the plutonium K-edge energy (E_k = 121.80 keV). As a result, the assay is somewhat sensitive to variations in the matrix properties. A two-source measurement using the ^{75}Se 121.1 keV and ^{57}Co 122.0 keV gamma rays, would decrease the matrix sensitivity while increasing the plutonium sensitivity.[29]

There is, however, an analytic technique which is useful for correcting the measured transmissions of lines which lie away from the K-edge energy, if medium or high Z matrix contaminants are present. Plots of log $\mu(E_\gamma)$ vs log E_γ are linear, with a slope m, over limited energy ranges for all Z. Figure 20 is a plot of m between 100 and 150 keV, as a function of Z.[27] Note that for $Z \gtrsim 50$, m is approximately a constant ($m \simeq -2.55$). If elements heavier than tin are present either in the sample or its container, the assay may be made relatively insensitive to their presence by extrapolating a transmission measured at energy E_γ, $T(E_\gamma)$, to that which would have been measured at the K-edge $T(E_k)$; i.e.,

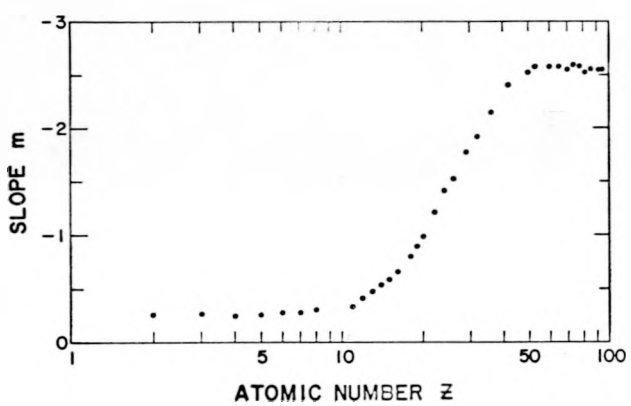

Fig. 20.
Slope m of log $\mu(E_\gamma)$ vs log E_γ between 100 and 150 keV plotted vs atomic number Z.

$$\log[-\ln T(E_k)] = \log[-\ln T(E_\gamma)] - 2.55 \log \frac{E_k}{E_\gamma} \quad .$$

An example of this procedure is summarized in Fig. 21. The ratios of transmissions of the ^{75}Se 136- and 121-keV gamma rays were measured through a plutonium-bearing solution (ρ_{Pu} = 67.5 g/ℓ) and a variety of tin thicknesses. The results are plotted as R vs the effective tin density, had it been distributed in the solution. The measured ratio R_m is strongly dependent on the density of the matrix contaminant. The ratio obtained from the corrected transmission values R_c varies by only 1.5% with the addition of tin equal to approximately 23 times the plutonium density.

Finally, note that densitometry measurements may be more conveniently made in a different geometry from that used for the SGS. If the transmission measurements are made along the cylindrical axis of the can rather than at right angles to it, the plutonium mass is given by

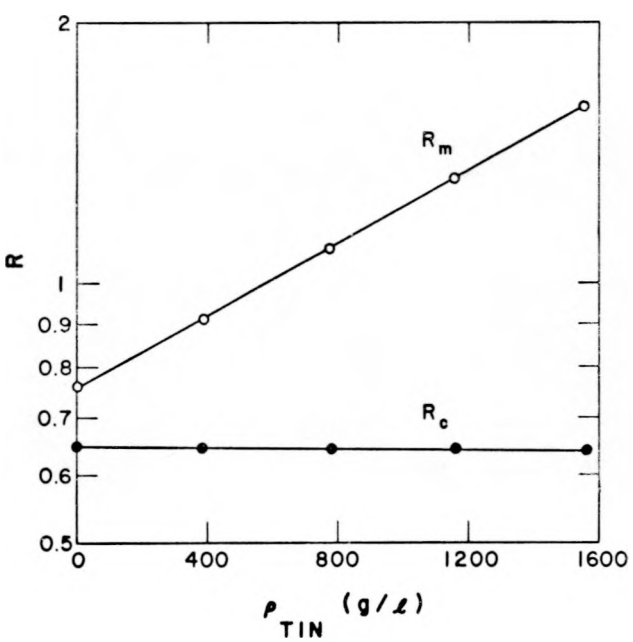

Fig. 21.
Logarithm of the measured ratio of the 136- to the 121-keV gamma-ray transmission R_m through a plutonium-bearing solution and the corresponding corrected ratio R_c plotted as a function of tin density in the solution.

$$M_{Pu} = \left(\frac{-\pi r^2}{\Delta\mu}\right) \ln \bar{R}$$

where $\bar{R}$ is the ratio of transmissions averaged over the can radius r. This has the advantage of being insensitive to the can fill height. A demonstration model of an instrument using this technique is under development.

2. L_{III}-Absorption Edge Techniques (T. R. Canada, W. B. Tippens, T. D. Reilly, and J. L. Parker)

The sensitivity of the densitometry assay technique is proportional to $\Delta\mu$, the change in the mass absorption coefficient across the absorption edge of the element of interest.[29] In the cases of uranium and plutonium, $\Delta\mu$ at the K-edge is approximately 3, limiting the technique to materials containing areal SNM densities of ≥ 0.2 g/cm^2. At the L_{III} edges of these materials $\Delta\mu$ is approximately 50, thus allowing the technique to be applied to lower plutonium and uranium densities.[27]

Figure 22a shows the x-ray spectra transmitted through several 1.97-cm-thick uranium solutions. These data were obtained using a 22-keV x-ray beam and a small Si(Li) detector. The uranium L_{III} edge is clearly seen. The logarithm of the ratio of the transmissions on either side of the edge is plotted as a function of the uranium density in Fig. 22b. The solid line is a least squares fit to the data of the function $R = A \exp(-B\rho_U)$ where A and B are the derived parameters. The fit parameters correspond to a $\Delta\mu$ between 16.92 keV and 17.48 keV (the points at which R was calculated) of 52.9 cm^2/g.

An alternate approach to reducing these data is to derive the uranium density by calculating the explicit shape of the spectrum. An example of this procedure is shown in Fig. 23. The points are the measured spectrum. The solid line is the calculated transmitted spectrum assuming an original 22-keV, tungsten target, bremsstrahlung spectrum, and a 1.97-cm-thick sample with a uranium density of 25.1 g/ℓ. The calculation includes a Gaussian averaging procedure which accounts for the finite detector resolution (270 eV FWHM). The calculation is seen to reproduce the measured shape reasonably well.

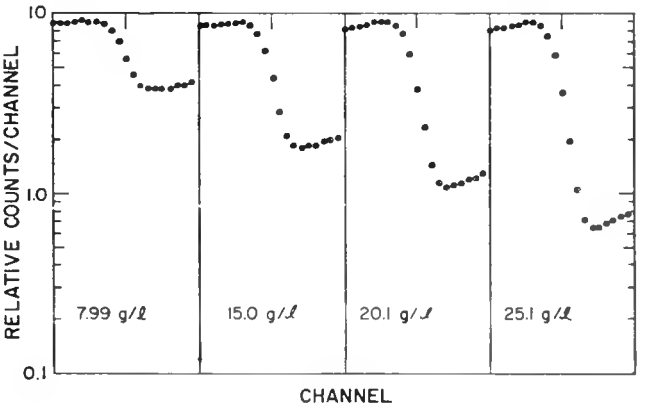

(a)

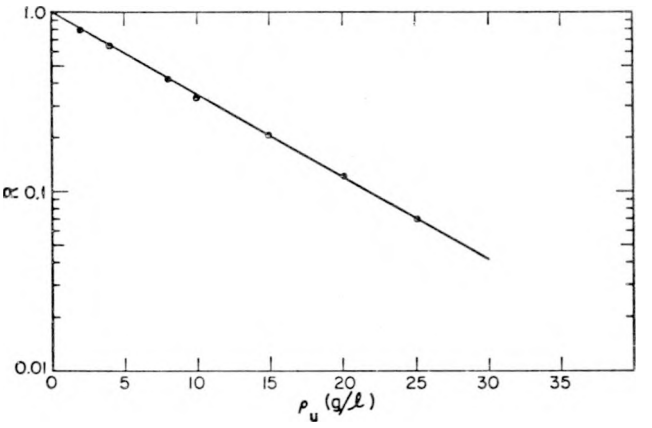

(b)

Fig. 22.
(a) X-ray spectra transmitted through solutions containing a range of uranium densities. (b) Logarithm of the ratio of the transmissions on either side of the L_{III} edge vs the uranium density. The solid line is a least squares fit to the data.

Programming is presently under way to perform a search for ρ_u to find that value which gives the best fit to a measured spectrum. This approach will have the advantage of using all the data about the edge to determine ρ_u and thus will reduce the required counting time.

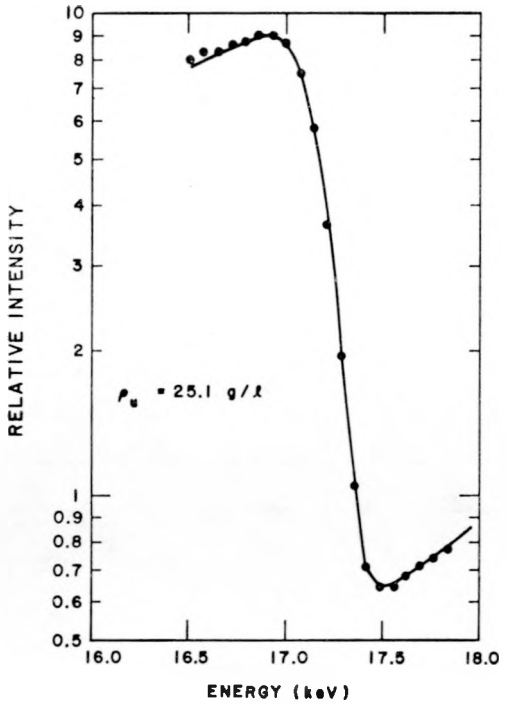

Fig. 23.
Comparison of a measured, transmitted x-ray spectrum (points) with that calculated (solid line).

H. An Accurate Determination of the Plutonium K-Absorption Edge Energy Using Gamma-Ray Attenuation (T. R. Canada, R. C. Bearse,* and J. W. Tape)

As part of the ongoing research and development program in safeguarding SNM, the mass attenuation coefficient μ for plutonium has been measured at a number of gamma-ray energies between 96.7 and 199.0 keV, with a view to determining the properties of the plutonium K-absorption edge.[29] Bearden and Burr[30] have listed the K-shell electron binding energy to be 121.818 ± 0.044 keV, and Veigele[31] has calculated the change in μ across the edge (the jump) to be 3.223 cm²/g. It was thus expected that the difference in μ determined with the gamma rays from ^{152}Eu (121.783 ± 0.009 keV[32]) and ^{57}Co (122.060 ± 0.010 keV[32]) would be nearly equal to the K-edge jump. However, the measured difference was approximately half the expected jump. Further tests indicated that the ^{152}Eu gamma-ray energy falls near the midpoint of the edge, thus allowing a rather accurate determination of the centroid of the plutonium K-absorption edge.

To determine $\mu(E_\gamma)$, the gamma-ray transmission through the sample (a 1N HNO_3, 227.7 ± 0.2 g/ℓ plutonium, polyethylene-encapsulated solution with a thickness of 1.97 ± 0.01 cm) was measured at 11 energies. These measurements were performed relative to an identical container of H_2O. The transmission differences between the water blank and the 1N HNO_3 solution, less than 1%, have been ignored. A schematic of the experimental arrangement is shown in the inset of Fig. 24. The detector was a 1-cm³, planar Ge(Li) with a resolution of about 600 eV at 122 keV. Standard, high-resolution electronics were used. Net photopeak areas were extracted from the spectra by subtracting a background obtained by averaging counts on each side of the respective peaks.

Mass attenuation coefficients were derived from these data by use of the relation

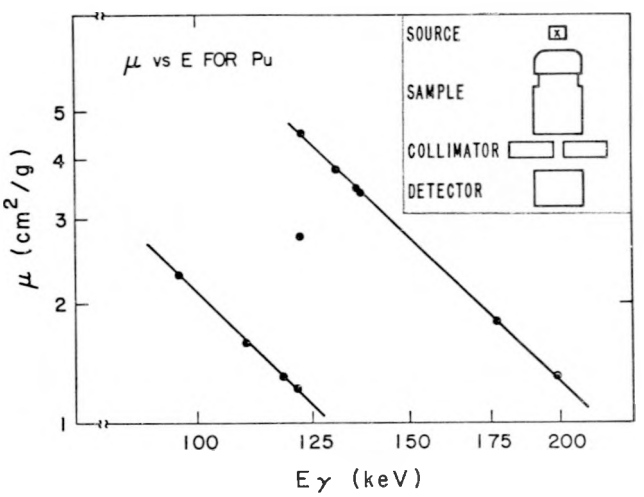

Fig. 24.
Measured mass attenuation coefficients plotted as μ vs E_γ on a log-log scale. The straight lines are least squares fits to the experimental data whose uncertainties are smaller than the symbols.

*University of Kansas.

$$\mu(E_\gamma) = \frac{-\ln T(E_\gamma)}{\rho_{Pu}X} \quad , \qquad (6)$$

where $T(E_\gamma)$ is the transmission measured at E_γ, and $\rho_{Pu}X$ is the areal plutonium density of the sample. The results are tabulated in Table VIII and plotted on a log-log scale in Fig. 24.

The measured $\mu(E_\gamma)$ and the K-edge jump are found to be in good agreement with the calculations of Veigele. As Table VIII indicates, the average deviation between the present results for μ and those of Veigele is 4% for energies below the edge and less than 1% for energies above the edge. The jump was obtained by fitting the data (in log-log form) on each side of the edge to straight lines and extrapolating each to an energy of 121.818 keV. (This energy choice is not critical. A ±100-eV variation changes the jump value obtained by ±0.2%.) The resulting fits are shown as solid lines in the figure. The jump was thus measured to be 3.22 ± 0.03 cm²/g, which is equal to Veigele's value of 3.22 cm²/g. Within experimental uncertainties, the jump determined by extrapolation is equal to the difference between the μ of the ^{75}Se (121.115 keV) and that of the ^{57}Co (122.050 keV) gamma rays, viz., 3.18 ± 0.03 cm²/g.

The μ measured for the 121.783 keV gamma-ray line in ^{152}Eu, 2.76 ± 0.03 cm²/g, lies approximately midway between those measured for the ^{75}Se and ^{57}Co lines. This may be a result of the finite width of the absorption edge (approximately 100 eV[33]), or it may be due to the presence of a previously unreported and unresolved doublet in ^{152}Eu at 121.783 keV, with energies straddling the edge. The latter possibility was investigated by measuring the transmission of the ^{152}Eu gamma ray through three plutonium-bearing solutions with ρ_{Pu} = 75.89, 151.8, and 227.7 g/ℓ. If the ^{152}Eu line were a doublet, the resulting data would be fit by a two-component exponential of the form

$$T = A \exp(-\mu_1\rho_{Pu}X) + (1 - A)\exp(-\mu_2\rho_{Pu}X)$$

where μ_1 and μ_2 are approximately the attenuation coefficient measured at 121.115 and 122.060 keV, respectively, and A is the fitting parameter. It was

TABLE VIII

GAMMA-RAY MASS ATTENUATION COEFFICIENTS OBTAINED FOR PLUTONIUM

Energy (keV)[a]	Source	This Work μ(cm²/g)	Calculated[b] μ(cm²/g)
96.733 ± 0.002	^{75}Se	2.29 ± 0.03	2.21
109.777 ± 0.010	^{169}Yb	1.65 ± 0.02	1.62
118.140 ± 0.015	^{169}Yb	1.41 ± 0.02	1.35
121.115 ± 0.003	^{75}Se	1.33 ± 0.01	1.27
121.783 ± 0.009	^{152}Eu	2.76 ± 0.03	—
122.060 ± 0.010	^{57}Co	4.51 ± 0.03	4.46
130.513 ± 0.010	^{169}Yb	3.80 ± 0.04	3.79
135.000 ± 0.005	^{75}Se	3.48 ± 0.03	3.44
136.471 ± 0.010	^{57}Co	3.41 ± 0.03	3.41
177.177 ± 0.010	^{169}Yb	1.83 ± 0.02	1.82
197.951 ± 0.020	^{169}Yb	1.41 ± 0.01	1.40

[a]Gamma-ray energies and their uncertainties are from Ref. 33.
[b]Interpolated from Ref. 32. The values include coherent and incoherent scattering. Veigele estimates his absolute uncertainties as 5-10%.

not possible to fit the data to this function; however, a single exponential with μ = 2.76 cm²/g fit the data well, ruling out the possibility that the μ we measure is due to a doublet at this energy.

It can be assumed therefore, that the 121.783-keV gamma ray falls on the edge, thus allowing a determination of the centroid energy E_k of the plutonium K-absorption edge. Two approaches have been used to obtain E_k. Both ignore the possibility of any structure that may be present on or just above the edge.[34,35]

In the first approach, the edge energy is defined to be that energy at which the plutonium mass-attenuation coefficient has a value equal to 2.92 cm²/g (the solid, horizontal line in Fig. 25), i.e., an average of those measured at 121.115 and 122.060 keV. Thus, the ^{152}Eu gamma-ray energy sets a lower limit on the edge energy. An upper limit is determined by drawing a straight line between the ^{57}Co and ^{152}Eu data points (the dashed line in Fig. 25) and determining the energy at which this line intercepts the horizontal line μ = 2.92 cm²/g. The limits obtained using this procedure are 121.783 ≤ E_k ≤ 121.804 keV.

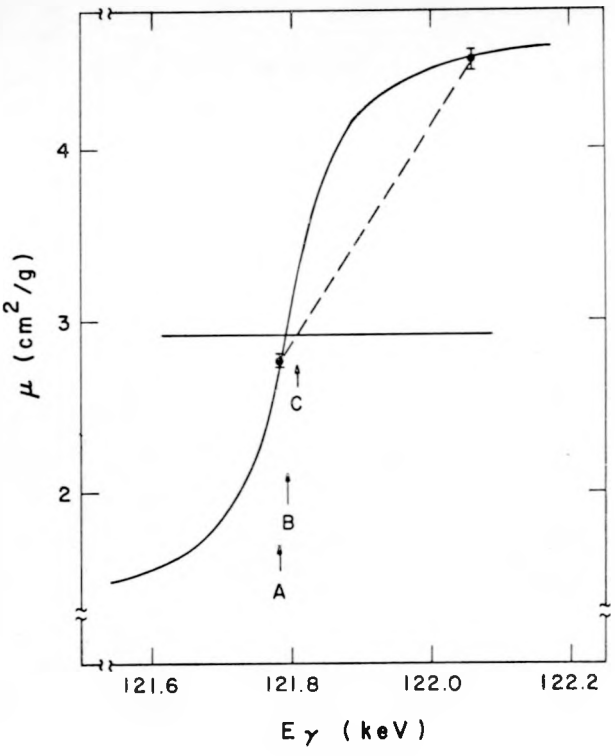

Fig. 25.
Expanded plot of μ vs E_γ in the immediate vicinity of the K-edge. The horizontal line is the average value of μ across the jump (2.92 cm²/g). The dashed line connects the data points at 121.783 keV (^{152}Eu) and 122.060 keV (^{57}Co) and determines the upper and lower limits of the edge energy, A and C, respectively. The curve is a plot of Eq. 7 which determines the edge energy B.

In the second approach, the edge shape is assumed (after Richtmeyer et al[36]) to be given by

$$\mu(E_\gamma) = \mu_0 + C\left[\frac{1}{2} - \frac{1}{\pi}\tan^{-1}\left(\frac{E_k - E_\gamma}{\frac{1}{2}\Gamma}\right)\right] , \qquad (7)$$

where E_k is the edge energy, Γ is the width (which we take to be 110 eV[33]), and μ_0 and C are constants. Using the values of μ obtained for gamma rays of energy 121.115, 121.783, and 122.060 keV, the constants in Eq. 7 are evaluated and a value E_k = 121.795 keV is obtained. The resulting curve is shown as a solid line in Fig. 25. Because the 121.783-keV gamma ray is so close to E_k, the latter is insensitive to changes in the parameters. For example, a 10% change in Γ produces only a 1-eV change in E_k.

On the basis of these estimates, we assign an energy of 121.795 ± 0.014 keV to the plutonium K-absorption edge (this includes the uncertainty of 0.009 keV in the energy of the ^{152}Eu gamma ray). This energy is consistent with the value of 121.818 ± 0.044 keV given in Ref. 33, but reduces the uncertainty by more than a factor of 3.

I. PDP-11/20 Computer System Upgrade (T. L. Atwell and W. B. Tippens)

Our existing PDP-11/20 minicomputer system located in Group R-1's gamma-ray spectroscopy laboratory has been recently upgraded to enhance the group's software development and data analysis capabilities. The system will now support up to three users on a time-sharing basis.

Hardware upgrades included: (a) the refurbishing of an existing Pertec 3100, dual 1.2-million word disk drive to which was added an International Memory System Model DM-100/Pertec, PDP-11 compatible controller (the upper, removable disk unit is now 100% media interchangeable with the standard RK-11 DEC pack disk cartridge); (b) the addition of an

RX-11 dual 128k word floppy disk unit; (c) the addition of 8k of core memory to bring the PDP-11/20 core storage up to 28k; (d) the installation of two ADM-1 interactive CRT display terminals to support two additional users; and (e) the addition of a 180-character/s line printer. Previously existing peripherals included a PC-11 Reader/Punch, a TC-11 Dual Dectape, a 4k Geoscience multichannel analyzer with dual 8192 ADCs, and a segmented gamma-ray scanner table. A block diagram of the complete PDP-11/20 system is shown in Fig. 26.

Software upgrades include the installation of a new RT-11 operating system (version V02C-02) and the addition of the FORTRAN IV and MU-BASIC programming languages. With the peripherals described above, running RT-11 in either a single job or foreground/background environment will now support up to three independent users in a number of configurations. The two most commonly used configurations are: (a) running MU-BASIC in the foreground for two users while a third user is running FORTRAN or doing assembly language program development (using EDIT, MACRO, LINK) in the background, and (b) running only MU-BASIC in the background for support of three users. In any of these configurations each user has access to any of the peripherals described above.

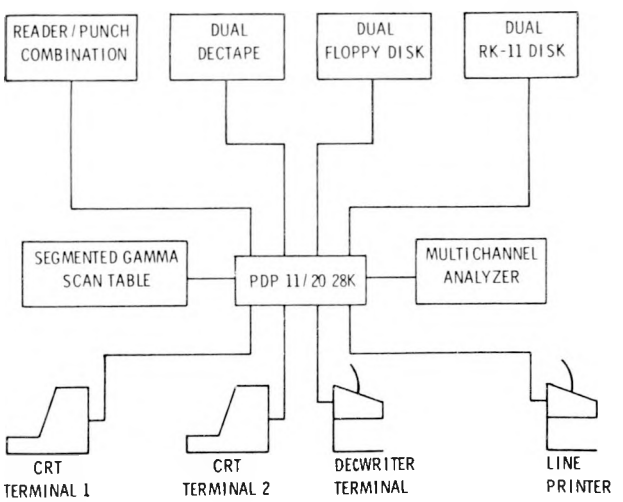

Fig. 26.
PDP-11/20 system configuration.

Installation of the dual floppy disk unit provides a very efficient, convenient, and inexpensive method of user program and data file storage. Floppy diskettes are thin, flexible, oxide-coated disks similar in size to a 45-rpm phonograph record. The disk itself is sealed in a 20- by 20-cm envelope which continuously cleans the surface as the disk rotates. Because of the relatively slow rotational speed (360 rpm), surface flexibility and constant cleaning action, the diskette is quite insensitive to dust and has proved to be extremely reliable. The floppy disk has a capacity of 128k words, offers an average file access time of 0.5 s, and transfers data at a speed of 18 μs per 8-bit byte.

J. Software Enhancements to MU-BASIC/RT-11 (T. L. Atwell)

The MU-BASIC/RT-11 language is currently being used for three of Group R-1's PDP-11 minicomputer systems that run in a multiuser environment. Several user routines have been written for MU-BASIC and a few internal source modifications have been made to enhance the time-sharing performance of the language.

Four user routines have been developed: (a) SPND(T) suspends execution of a user's program for a specific time T ($1/60 \leq T \leq 10^7$ s); (b) EXNO(X) sets the number of statements X to be executed per user ($0 < X < 128$) before time-sharing with another user; (c) PRIO(X) allows the user to dynamically alter his execution priority ($0 < X < 128$); and (d) TIMR(N,X,T) provides each user with N timers, each of which will set variable X to 1 after the specific time T has expired ($1/60 \leq T \leq 10^7$ s).

The SPND routine is especially useful in situations where a user spends a lot of computer time looping through the same subprogram testing for instrumentation timeouts or requests from peripheral units. In such a looping situation, without the SPND routine, that user would require a percentage of unavailable computer time equal to 100% divided by the number of users. To demonstrate the computer time that the SPND routine can save, assume that it takes only 0.05 s to run through a program loop which requires execution only once every 10 s. In a two-user environment, when user A inserts the SUSP(600) command at the end of his loop, he will be using only 0.5% of the available computer time, leaving user B with 99.5%.

K. Delayed-Neutron Energy Spectra (M. S. Krick and A. E. Evans*)

Equilibrium delayed-neutron energy spectra have been measured from the fast fission of ^{235}U, ^{238}U, and ^{239}Pu. The experimental procedure and preliminary results have been reported previously (Ref. 14, p. 9).

The final delayed-neutron spectra are shown in Fig. 27. Energy peaks observed in the spectra are tabulated and compared with previous work in Table IX. The average delayed-neutron energies,

*Group R-5.

TABLE IX

DELAYED-NEUTRON PEAK ENERGIES (keV)

Present Work					
^{238}U	^{239}Pu	^{235}U	Shalev and Cuttler[a]	Sloan and Woodruff[a]	Chulick et al[a]
—	—	—	—	33	—
—	—	—	—	41	—
—	—	—	—	60	—
68	68	68	75	76	—
90	—	—	—	90	95
—	—	—	—	103	104
130	133	125	125	129	135
—	—	—	170	161	158
183	183	178	180	183	188
—	—	205	—	210	205
—	—	—	—	—	225
263	255	255	255	240	240
—	268	268	—	283	265
—	310	—	320	—	—
—	330	—	325	—	—
345	—	343	355	351	340
378	375	370	375	—	—
—	—	380	390	—	—
—	—	418	420	420	430
—	—	—	440	—	—
480	475	488	480	467	—
500	500	503	500	—	—
560[b]	560[b]	560[b]	570	552	—
—	—	610	—	—	—
—	—	—	680	—	—
—	713	—	—	—	—
760[b]	762	753	750	—	—
852[b]	845	858	850	—	—
945[b]	—	958	950	—	—
—	1 150[b]	1 160[b]	1 145	—	—
1 173	—	—	—	—	—
1 200	—	—	—	—	—

[a]Data for ^{235}U taken from Ref. 38, Table VI.

[b]Multiple peak.

TABLE X

AVERAGE DELAYED-NEUTRON ENERGIES

Isotope	Average Delayed-Neutron Energy (keV)
^{235}U	457
^{238}U	542
^{239}Pu	509

corrected for the presence of fission neutrons resulting from multiplication in the sample, are listed in Table X. A detailed description of the entire experiment will be published elsewhere.[37]

L. Nondestructive Assay Training Program (T. R. Canada, J. L. Parker, and J. W. Tape)

The LASL-ERDA NDA training program course, "Gamma-Ray Spectroscopy for Nuclear Material Accountability," was conducted by Group R-1 in Los Alamos from May 17-21, 1976.

Demand for the courses offered in the training program continues to be high. For this particular course, enrollment was originally limited to 20 participants but was increased to 25 to accommodate more of the 35 who applied. As shown in Table XI, participation spanned the national and international safeguards community. The mix of ERDA, NRC, IAEA, national laboratory, and private industry personnel provided a stimulating environment for both the laboratory exercises and informal technical exchanges.

The course stresses the powerful NDA techniques available for SNM assay using high-resolution gamma-ray detectors.[39] Nine staff members of Group R-1 gave general lectures and demonstrations, and instructed small laboratory groups of four to five participants. Figure 28 shows one of the instruction sessions.

Since the formal training sessions began in 1973, 116 people have attended the courses on NDA fundamentals and advanced gamma-ray spectroscopy (see Table XII). Interest in these two courses remains high and they will continue to be offered in future years.

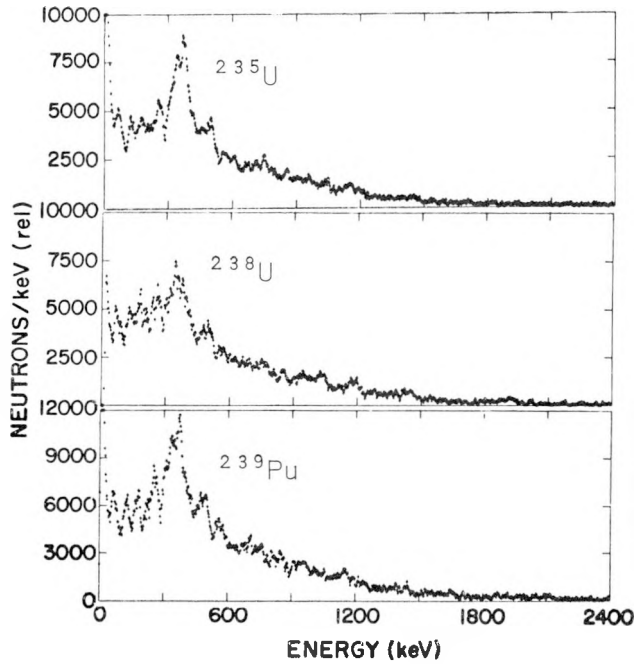

Fig. 27.
Delayed-neutron spectra from ^{235}U, ^{238}U, and ^{239}Pu.

Fig. 28.
LASL instructor, Jack Parker, discusses a problem with a group of participants.

In 1976-1977 the program curriculum will be expanded from two to four courses (see Table XIII for the syllabus), each of which will be offered once a year. The courses, "Fundamentals of Nondestructive Assay Using Portable Instrumentation" and "In-Plant Nondestructive Assay Instrumentation" will be offered during the weeks of November 1-5 and December 6-10, 1976, respectively. The remaining two courses are tentatively scheduled for the spring of 1977. Over the last 3 yr, this training program has proved to be an effective method of transferring laboratory-developed NDA technology to the diverse safeguards community. We believe that the expanded curriculum will help meet the growing needs of this community.

TABLE XI

GAMMA-RAY SPECTROSCOPY COURSE ATTENDEES

Organization	Representative
UK Atomic Energy Authority	A. S. Adamson, England
IAEA	Benson Agu, Nigeria Andrej Janikowski, Poland Chia-shi Lin, China (Taiwan) Demetrius Perricos, Greece Teodor Rosescu, Rumania Saurabh Sanatani, India
US ERDA	Stephen M. Baloga Ray Lux Craig S. Smith
National Bureau of Standards	B. Stephen Carpenter
Oak Ridge National Laboratories	M. M. Chiles
Oak Ridge Gaseous Diffusion Plant	Eugene E. Clark
US NRC	Anthony T. Gody Daniel J. Holody, Jr. Edward G. Selleck E. Thomas Shaub Philip Ting
Goodyear Atomic Corp.	James R. Griggs
Battelle Pacific Northwest Laboratories	Clark O. Harvey
Babcock & Wilcox	Ronald C. Hoffman D. Sherrill
Atlantic Richfield Hanford Co.	Cecil H. Kindle
General Atomic	Terry D. Metzgar
Lawrence Livermore Laboratory	Nicholas J. Roberts

TABLE XII

NDA TRAINING PROGRAM

Year	Course	Participants		
		US	IAEA and Foreign	Total
1973	Fundamentals of NDA using portable instrumentation	20	—	20
	Individual training (advanced NDA)	3	—	3
	1973 Total			23
1974	Fundamentals of NDA using portable instrumentation	20	3	23
	Individual training (advanced NDA)	5	—	5
	1974 Total			28
1975	Fundamentals of NDA using portable instrumentation	14	13	27
	Gamma-ray spectroscopy for nuclear material control	19	2	21
	Individual training (advanced NDA)	4	3	7
	Off-site training (IAEA and nuclear industry)	—	16 50	66
	1975 Total			121
1976 (spring)	Gamma-ray spectroscopy for nuclear material control	18	7	25

TABLE XIII

CURRICULUM FOR NDA TRAINING PROGRAM

1. Fundamentals of Nondestructive Assay Using Portable Instrumentation

A survey of passive gamma-ray and neutron SNM assay techniques, including detector characteristics and operation procedures. Topics include enrichment measurements, corrections for sample self-attenuation of gamma rays, quantitative plutonium assay, neutron scattering, and the measurement of plutonium metal buttons, mixed-oxide fuel rods, and UF_6 cylinders.

2. Gamma-Ray Spectroscopy for Nuclear Material Accountability

A study of the applications of high-resolution gamma-ray spectroscopy to the NDA of uranium- and plutonium-bearing materials. Topics include: general techniques of high-resolution spectroscopy, differential gamma-ray absorption, transmission correction factors, and gamma-ray densitometry. Demonstrations of automated systems are given.

3. In-Plant Nondestructive Assay Instrumentation

An in-depth study of the capabilities and limitations in practical plant situations of the neutron coincidence counter, Random Driver, transmission-corrected segmented gamma-scan system, and a passive gamma-ray solution analysis system. The instruments are available with emphasis on hands-on experience coupled with a sound understanding of the generic instrument types.

4. Integrated Nondestructive Assay Systems—Concepts and Implementation

An overview of real-time dynamic materials accounting and control concepts and the techniques for their incorporation into practical safeguarded plants. Topics include methods of defining material balance areas, process line modeling and simulation for the purposes of performance evaluation, possible impacts on process operations and a brief survey of available NDA instrumentation. Examples of the implementation of an integrated safeguards system including computer/information subsystem are drawn from the DYMAC project.

PART 2
DEVELOPMENT AND DEMONSTRATION OF DYNAMIC MATERIALS CONTROL—DYMAC PROGRAM
(R-Division, CMB-Division, and E-Division Staffs)

I. CONCEPTS AND SUBSYSTEM DEVELOPMENT

A. NDA Instrumentation

1. Load Cell Weighing System (V. S. Reams, T. Gardiner, W. R. Severe, M. M. Stephens, and C. O. Shonrock)

A load cell weighing system has been proposed as part of DYMAC at DP Site to implement an assay necessary for a material balance around the ash-leach process. The weighing system will enable DYMAC to take advantage of electronic data processing in maintaining material balances and thereby ensure that the measurements are timely, accurate, and digital. Furthermore, the use of a modified industrial measurement system (load cell with a digital scale) minimizes instrument design time, yields digital outputs, offers high transducer linearities (0.1-0.5% full scale), provides real-time measurements (0.1-2 s), and lowers human error.

A volumetric approach is feasible but would require human interaction to convert observed volumes to digital data via terminal entry. Transducers to replace this method of measurement are not readily available, not accurate enough, nor are they processor-compatible. For these reasons, volumetric measurements were not given serious consideration.

A weight approach likewise entails some problems, in particular, the highly corrosive environment inside the ash-leach gloveboxes where the weighing system is to be installed. To minimize corrosion, the load cells are constructed with a stainless steel case and strain structure. On the inside, the load cells are sealed and the strain gauges coated during manufacture. Strain gauge load cells have no moving parts, thereby eliminating the need for oil and dirt seals.

The load cell weighing system is composed of five assemblies as shown in Fig. 29. The BLH-U2M1 load cell* (which has a 45-kg capacity) and the suspension rigging (shown in Fig. 30) provide a means to raise the column approximately 1 cm off the floor of the glovebox, make a weight measurement, and return the column to its resting position on the glovebox floor. Stainless steel components are used wherever possible because of the corrosive atmosphere. The load cell assembly is the only part of

BLH Electronics, Inc., Waltham, MA.

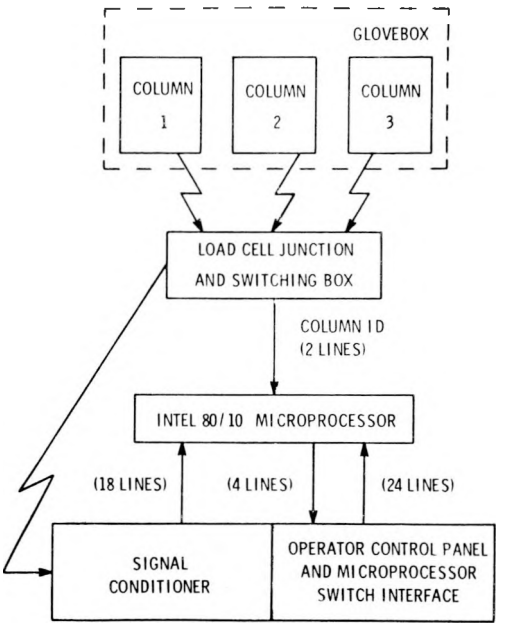

Fig. 29.
Load cell weighing system.

the weighing system subject to contamination and chemical corrosion; all other assemblies are remote to the glovebox.

The second assembly is the load cell junction and switching box. The full system at DP Site will have three columns to weigh, only one of which will be ready to transfer at a given time. Thus, three assemblies like that shown in Fig. 30 will be located in a single glovebox line. The junction box will select the load cell connected to the column to be weighed and send that signal to the rest of the instrumentation. Column selection is done with a three-position rotary switch mounted on the front panel of the junction box. This selection switch also provides a 2-bit binary code for use by the instrumentation in identifying which column is to be weighed.

Third is the signal-conditioning electronics (BLH-450 Transducer Indicator*) which contains circuitry that scales and amplifies the small load cell voltages and presents them to a digital panel meter (DPM) which displays a digital value while providing analog-to-digital conversion to a rear panel connector [4-1/2 digits binary-coded decimal (BCD), full parallel, and compatible with transistor-to-transistor logic (TTL)]. Refer to Fig. 31 for a detailed drawing of the front panel. There are several front panel adjustments for full-scale and zero adjustment which are not normally available to the operator, as they are used only during system calibration. These controls and the DPM are covered by a Plexiglas panel and take up half the width of a standard 19-in. rack panel.

Fourth is the operator control panel and microprocessor switch interfacing electronics (shown in Fig. 31). The operator control panel has three pushbutton switches (PBSW) [SEQ., ERROR-RESET, SEND W.], five light-emitting diode (LED) indicators [SEQ READY, READY, INITIAL W. COMP., FINAL W. COMP., ERROR RESET], and a four-digit LED display [WEIGHT]. The three LEDs [READY, INITIAL W. COMP., FINAL W. COMP.] are used by the instrumentation to inform the operator of the present step in the weighing sequence. The two LEDs [SEQ. READY, ERROR RESET] inform the operator which of the

BLH Electronics, Inc., Waltham, MA.

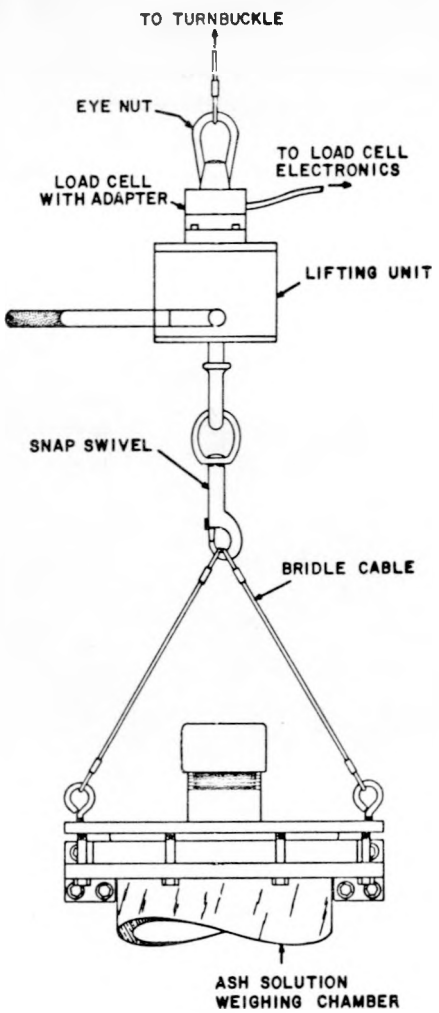

Fig. 30.
Single cell tension system.

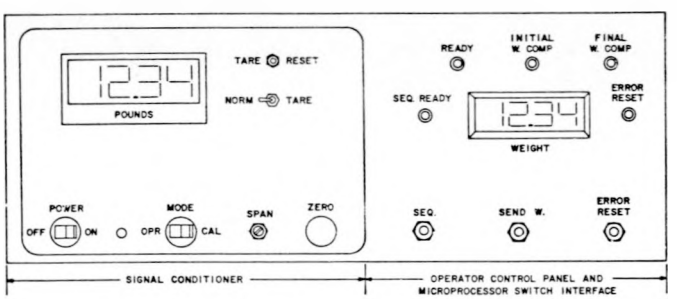

Fig. 31.
Signal conditioner and operator control panel for load cell weighing system.

corresponding PBSWs [SEQ, ERROR RESET] is active. The SEND W. PBSW is active only when the WEIGHT display has information displayed. The switch interface electronics provide a latching mechanism for the PBSWs and a selective enable of these latches under microprocessor control. Current buffers between the microprocessor and LEDs are provided along with suitable power supplies for the logic and LEDs.

Fifth and final is the microprocessor (Intel 80/10) assembly which consists of a front panel with pilot light, fuse, and ON-OFF switch, a single board computer system; and power supplies.

The microprocessor hardware accepts 16 bits of data from the DPM [4 BCD digits] and an 8-bit status word composed of 2 bits from the DPM [overflow and sign], 4 bits from the switch interfacing electronics [SEQ, ERROR-RESET, SEND W., and a spare], and 2 bits from the load cell junction box [column identification 2^0, 2^1].

The hardware sends 16 bits of data to the LED display [4 hexadecimal digits] and an 8-bit instrument control word which consists of 2 bits for processor status [initial weight sign bit, spare], 4 bits of switch enable to the switch interface electronics [SEQ enable, ERROR-RESET enable, SEND W. enable, and spare enable] and 2 bits of LED control [READY, INITIAL W. COMP.] to the operator panel. Note that SEQ enable is displayed on the SEQ READY LED, ERROR-RESET enable on the ERROR-RESET LED, and SEND W. enable on the FINAL W. COMP. LED (all LEDs are on the operator control panel).

The microprocessor software provides weighing sequence control, weight calculation, error detection, and data output. The last function is implemented with a serial data port which is software- and hardware-programmed for 300-baud, 20-mA current loop transmission to the DYMAC-Nova 840 at DP Site. Initiation of this transmission is via the SEND W. PBSW.

The assay for the ash-leach process depends on three separate measurements. First, an ash-leach column is sampled before transfer of fluid to a 60-ℓ tank (where material is stored awaiting the ion-exchange process). The weight of this sample, W_s, is determined with an electronic balance. Second, the amount of plutonium in the sample is determined by means of gamma-ray measurement (Pu_s). Finally, the weight of fluid actually transferred from the column (W_c) is determined by means of a load cell weighing system attached to the column. The procedure is to make a difference measurement, that is, column weight after fluid transfer subtracted from column weight before fluid transfer. If all three measurements are available, then the amount of plutonium transferred (Pu_c) is calculated according to the following formula:

$$Pu_c = Pu_s(W_c/W_s) .$$

This method differs from the method presently used at DP Site which measures volume instead of weight, that is,

$$Pu_c = Pu_s(V_c/V_s),$$

where V_c is the volume of fluid transferred from the column, V_s is the volume of sample used to determine the plutonium content of the fluid, and Pu_s is the amount of plutonium measured in V_s.

If the weighing system can be made environmentally compatible, then the primary problems are long-term stability, measurement reproducibility, and in-box calibration procedures. To explore these problems, a microprocessor-based evaluation system was used to simulate the measurement sequences. A microprocessor was chosen for convenience and to familiarize Group R-1 personnel with the capabilities of such a unit as an instrumentation subassembly with an eye towards solving some instrumentation problems at the new plutonium facility (TA-55). Table XIV summarizes the evaluation as it pertains to reproducibility and stability of the load cells. Certain conclusions can be drawn from the table: (a) the bias is not significant, (b) there are no obvious long-term trends, (c) the relative random error

$$\sigma_\varepsilon^1 = \frac{s(w_j)_p}{\bar{\bar{w}}} = 0.03\% \quad ,$$

(d) the long-term systematic error (relative)

$$\sigma_\delta' = \frac{\left[(\bar{\bar{w}}-w_0)^2 + s^2(\bar{w}_j)/m + \Delta^2/6\right]^{1/2}}{\bar{\bar{w}}} = 0.02\% \quad .$$

These evaluations illustrate the out-of-glovebox capabilities of these instruments: the data will form a baseline for comparison with data to be taken in

TABLE XIV

LOAD CELL EVALUATION

Sample Number	$\bar{w}_j$[a] (g)	$s(w_j)$[b] (g)	$s(w_j)_p$[c] (g)	$\bar{\bar{w}}$[d] (g)	$s(\bar{w}_j)$[e] (g)	$(\bar{\bar{w}}_j - w_0)$[f] (g)
1	12 276.68	4.54	4.54	12 276.68	—	−2.11
2	12 275.55	2.27	3.41	12 276.12	0.77	−3.24
3	12 289.16	4.34	3.72	12 280.46	7.56	10.37
4	12 277.82	2.27	3.36	12 279.80	6.31	−0.97
5	12 275.55	2.27	3.14	12 278.95	5.79	−3.24
6	12 272.15	2.62	3.05	12 277.82	5.88	−6.64
7	12 275.55	5.71	3.43	12 277.49	5.42	−3.24
8	12 286.89	2.27	3.29	12 278.67	6.02	8.10
9	12 277.82	4.34	3.40	12 278.57	5.65	−0.97
10	12 278.95	0.00	3.06	12 278.61	5.32	0.16
11	12 277.82	4.34	3.18	12 278.54	5.05	−0.97
12	12 277.82	7.75	3.56	12 278.48	4.82	−0.97
13	12 268.75	6.80	3.81	12 277.73	5.35	−10.04
14	12 275.55	2.27	3.70	12 277.58	5.19	−3.24
15	12 272.15	2.62	3.63	12 277.21	5.18	−6.64
16	12 290.29	4.54	3.68	12 278.03	5.98	11.50
17	12 277.82	4.34	3.72	12 278.02	5.80	−0.97

[a]Average for four weighings.
[b]Standard deviation of the same four weights.
[c]Pooled standard deviation (cumulative).
[d]Cumulative average.
[e]Standard deviation of average ($\bar{w}_j$) values.
[f]Bias, w_0 = 12 278.79.

the glovebox after installation at DP Site. Postinstallation data can be obtained by system calibration checks using in-box dead-weight standards.

Two types of load cell systems have been considered: a compression system which requires multiple cells (see Fig. 32) and a modified base plate under the column, and a tension system which uses a single cell and a lifting mechanism to facilitate column suspension during weighing (see Fig. 30). In view of lowered cost, less susceptibility to damage from spills, simpler in-box set-up procedure, improved transducer accuracy, and minimum in-box electrical connection, the tension approach is being pursued.

2. Standards and Measurement Control (W. R. Severe and R. Siebelist)

A standards and measurement control program has been initiated at DP Site. It is intended that this program provide a data base for evaluation of the measurement program as well as experience in measurement control methods. The standards and measurement control program is expected to (a) develop an adequate series of well characterized standards; (b) implement written procedures necessary to formalize methods of calibration and equipment operation; (c) determine measurement accuracies and precisions; (d) ensure and document

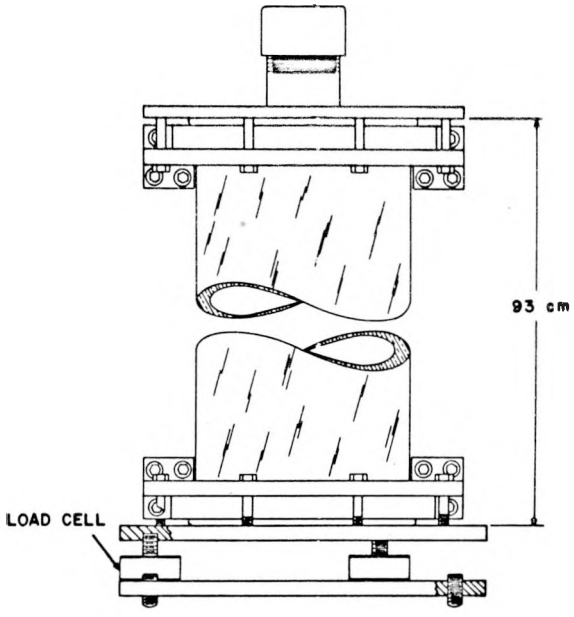

Fig. 32.
Multiple cell compression system.

proper performance of gamma-ray counters, neutron counters, and weighing devices; and (e) establish a continuing program of administrative review and assessment.

Presently, effort centers on the DP Site counting room where NDA of a number of different solid material types is conducted using both gamma-ray counting and neutron counting procedures. Calibrations will be made using a linear regression of several standards that cover a range of plutonium values. Control charts will be generated to monitor instrument precisions and accuracies. Measurements of process material will be used to construct the control chart for precision. This chart will make use of an "F test"[40] to ensure that instrument precisions are in control using the 95% confidence level as warning limits and the 99% confidence level as action limits. Accuracy will be tested by the daily measurement of reference standards. The control chart for accuracy will use the "t" distribution to test the hypothesis that, for a given calibration, the measured value of the standard is not significantly different from its known value. Control parameters are the 95% confidence level as warning limits and the 99% confidence level as action limits.

Currently the segmented gamma scanner and the 2-ℓ thermal-neutron coincidence counter are being evaluated using a series of specially prepared plutonium standards. A technique using linear regression and analysis of variance has been introduced to evaluate the performance of these instruments over a range of plutonium values and matrix compositions.

In the final system at TA-55, the central computer system will monitor and execute the measurement control program in real time, requiring control measurements at prescribed intervals. The standards and measurement control program is central in assuring that accurate, reliable[40] data are being supplied to the real-time accountability system.

B. Data Acquisition

Communication System (T. Gardiner, R. F. Ford,* and V. S. Reams)

The basic DYMAC configuration will consist of a network of instruments and terminals that communicate with a central computer. Different types of instruments and terminals will be used. The quantity of data sent by a given instrument to the computer will be small; likewise, computer signals to the instruments will consist of only a few control characters. Thus, there will be no need for high-speed communication links with DYMAC instruments. Instead, emphasis for these communication links is on reliability because system integrity depends on the assay value obtained by the instrumentation.

The terminals send the computer data which consist of transaction information entered by plant technicians when materials are moved or when they undergo chemical or physical change. The volume of data from the terminals will be greater than that from the instruments; however, data transmission rates will be governed by the technician's ability to enter data at a keyboard. The computer will send voluminous data to the terminals, consisting of prompts and messages to the technician and structuring for transaction entries. By using CRT display and high-speed communication techniques for these links, the transaction process can be accomplished expeditiously with a minimum amount of technician boredom and frustration.

**Group E-5.*

For the communication aspect of the DYMAC system we have concluded that serial-by-bit transmission over twisted pair transmission lines represents a reliable and cost-effective approach. The transmission lines will be driven by balanced, bipolar drivers located at each instrument and terminal, and at the computer. Character representation will conform to the American Standard Code for Information Interchange (ASCII) and will consist of a seven-bit character, an even parity bit, one start, and one stop bit. The interfaces between instruments, terminals, computers, and the communication equipment will be as defined by the Electronic Industries Association Standard RS-232-C. Different transmission rates will be used to accommodate the requirements discussed above. The rate for all instruments and for a few nonCRT terminals will be 300 baud, 1200 baud for CRT terminals, and 9600 baud for a few special cases where line printers are used to allow high-speed data listing.

The basic system, as described, is widely used and well understood. Standard commercial equipment is available for implementation. The system's flexibility will allow easy modification to accommodate techniques and equipment that we will develop to enhance reliability. In the near future we shall begin reliability enhancement studies.

C. Data Base Management (R. F. Ford,* J. Hagen, and C. Slocomb*)

Two types of data base management software packages are commercially available for minicomputers used in real-time accounting systems. The first type is a version of a software program (e.g., TOTAL, originally written to run on a large machine) which has been rewritten for a specific minicomputer. The second type is a software package available from the minicomputer manufacturer consisting of subroutines that allow the user to tailor-make a data base management system for a specific application.

The first type of software package, although very powerful, is nonetheless restrictive, particularly in the area of file structure definition. The second type of software package, although requiring more programming support within the user organization during system design and debugging, is flexible enough to accommodate the operating environment of a multiprocess plant with dynamic nuclear materials management and reporting requirements. Because of this need for flexibility, the DYMAC program has chosen the second approach.

D. Real-Time Accountability (D. D. Cobb and D. B. Smith)

The capability to model the flow and control of nuclear material through a facility such as TA-55 has been developed by Group R-1 (Ref. 41, Sec. IV and Appendix D). In the model, a schedule of material flow events is specific for each unit process, including an initial event in which beginning inventories are set, a minimum of one type of process event, and a final event in which runouts and cleanups are performed. Process descriptions and unit process event schedules are incorporated in a computer program called MOXSIM that simulates baseline plant operation 1 week at a time. MOXSIM uses the executive of the GASP IV simulation language to schedule the individual unit process events in proper sequence. The GASP IV controller provides added flexibility. In addition to timed events, it can schedule conditional events that arise during process operation, for example, stopping the flow of material when a tank has been filled.

The simulated process operation is defined in terms of true material flow data from each event. These data are saved for use by the measurement simulation computer program MACSIM which applies simulated measurements to flow data to produce measured material balance data.

Operation of the material control system is evaluated using the Monte Carlo computer code MACSIM (Material Accounting and Control Simulation) to simulate measurement of the true material flow data generated in MOXSIM, and compute material balances and cumulative summations (cusums) of material balances appropriate to each of the unit processes considered.

MACSIM incorporates a generic measurement model that has provision for both proportional and

---

*Group E-5.

constant random error components and for a constant bias term.* The measured value M of a true quantity μ is given by

$$M = \mu(1 + \eta) + \epsilon + \beta \quad , \tag{8}$$

where η and ϵ are the proportional and constant random errors, respectively, and β is the bias. The variance σ^2_M of M is given by

$$\sigma^2_M = \mu^2\sigma^2_\eta + \sigma^2_\epsilon \quad , \tag{9}$$

where σ^2_η and σ^2_ϵ are the variances of η and ϵ respectively. The random errors η and ϵ are each assumed to be normally distributed with mean zero. Individual measurement results are assumed to be independent.

Standard deviations σ_η and σ_ϵ are specified for each measurement situation. Because measurement uncertainty in a weighing operation is relatively constant over the range of the instrument, only σ_ϵ is given a nonzero value for mass determinations using either balances or load cells. In contrast, the uncertainty of an NDA measurement tends to be proportional to the quantity of material being measured, and only σ_η is assigned a nonzero value for this type of measurement. Furthermore, because the plant is expected to have an effective, operating measurement control program (which is designed to eliminate sources of measurement bias, or to estimate the effects of potential sources of bias and correct measurement data as needed), the bias term β in Eq. (8) is set to zero for all measurements.

NDA measurements are assumed to directly produce a value for the quantity of plutonium element present. The uncertainty in the plutonium isotopic composition and instrument calibration are incorporated into the imprecision (σ_η) specified for each NDA measurement. In the case of a weighing operation, the measured weight is multiplied by an element factor (grams of plutonium per gram of sample) to obtain the plutonium mass. The element factor is determined by chemical analysis of samples taken during plant operation. In MACSIM, the element factor is obtained by simulated measurement, using the uncertainty appropriate to the chemical analysis. The assigned uncertainty includes both analysis errors and sampling errors.

Each material balance computed in MACSIM is a linear combination of measured quantities of plutonium. The uncertainty in the computed value of the material balance is produced by the combined effects of uncertainties in the contributing measured values. In MACSIM, the measurement results are assumed to be independent, and the variance associated with each material balance is the sum of the variances of the terms in the material balance equation.

A cusum is computed by MACSIM after each material balance period. It is the sum of all material balances for the unit process since the beginning of the accounting period. The cusum variance is a complex combination of the variances of individual material balances, as these balances usually are not independent. In most unit processes, there are one or more variables for which a single measurement value appears as output in one material balance period (i.e., this value has a negative sign in the material balance equation) and as input in the next. For example, this can be the result of accumulating material in a tank or scrap container and measuring the contents during each balance period. In such cases, only the first and last measurements of the container contents appear in the cusum, and only the corresponding variances appear in the cusum variance.

The MACSIM code is sufficiently versatile to permit independent investigation of materials control sensitivity as a function of process variability, measurement variability, and instrument configuration. To date, the model has been used to evaluate the materials measurement and accounting system of a conceptual mixed-oxide plant of the future. The specific input information describing the new LASL plutonium facility is being prepared so that the modeling techniques can be applied to TA-55. Fixed sets of measurements will be applied to different sets of material flow data, and a variety of measurement strategies applied to fixed sets of flow data. Design choices will be based on the dual criteria of satisfactory sensitivity to both single-theft and long-term diversion and minimal perturbation of anticipated process operation.

**Statistical terms are used in accordance with American National Standard ANSI N15.5-1972, Statistical Terminology and Notation for Nuclear Materials Management.*

II. DYMAC IMPLEMENTATION

A. DP Site Test and Evaluation Phase

A major portion of the effort in the test and evaluation phase of DYMAC is directed towards the installation and operation of a prototype terminal system which will draw a nuclear material control balance around a unit process. For this demonstration the ash-leach process has been selected. Material flow and NDA measurement points are shown in Fig. 33.

In addition to the NDA measurement stations, four interactive terminals will be located in the process areas. Through these terminals process operators will enter transaction information which will be organized in files structured for a Nova 840 computer system to draw the material balance. In return, the terminals will provide production information to the operators. (For a more detailed explanation of the ash-leach process, see Ref. 14, p. 15.)

1. Computer Installation and Accounting System at DP Site (R. F. Ford,* J. Hagen, C. Slocomb,* A. Dross,** R. Wagner** T. Short,** and T. Gardiner)

The Nova 840 computer will handle data acquisition and accounting functions for the DP Site evaluation phase. To date, most of the effort has gone into producing a code which will emulate the present LASL accounting system with the additional feature of interactive terminal input. That code is operative and effort is now being directed towards accepting measurement data directly from the NDA instrumentation.

The present LASL accounting system records the movement and processing of nuclear material on a transaction sheet. This sheet is sent for keypunch conversion to cards and run on a batch basis at LASL's central computer facility. To verify the accuracy of the new terminal-based DYMAC code, both systems are being run in parallel. The results to date have been very good. For example, 1412 transactions were made during the last half of August and 1412 transactions were made on the DYMAC system. A comparison of results with the concurrent systems showed 35 differences, for a 97.5% correlation. Of these 35 differences, 30 were found to be caused by transaction sheets not being delivered to the DYMAC system; three were caused by undetected errors in data entry; two were program difficulties that will be corrected. If the 30 missing transactions are removed from the list of differences there are only five errors out of 1412 transactions for a 99.6% correlation.

Although the terminal-based system reproduces the functions of the present system, there are important differences due to the real-time nature of the terminal system. For example, the terminal system performs diagnostic checks on incoming terminal information before it is stored in the inventory file. In this way, incorrect information is kept out of the inventory file where it could trigger a false alarm or mask a loss of material. Most important, the real-time feature makes information available at any time.

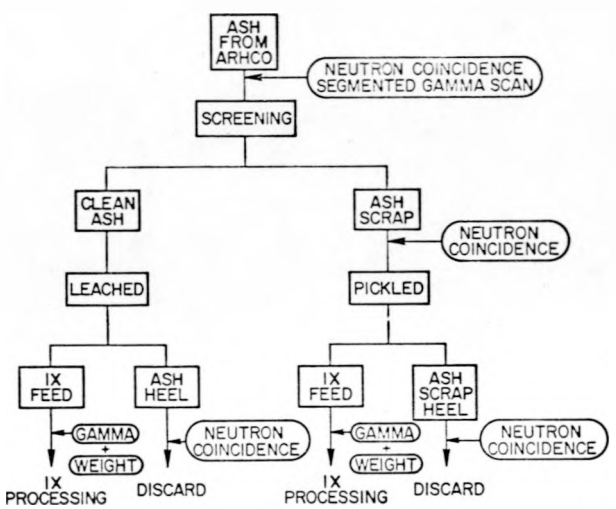

Fig. 33.
Flow diagram of ash-leach process showing NDA measurement points.

*Group E-5.
**Group CMB-11.

The next step in the DP Site evaluation will be to connect assay instruments to the central computer and operate them in conjunction with transaction terminals. This will allow us to close the loop around a unit process and closely simulate actual operation as it is planned for the new plutonium facility.

Several tentative configurations for terminals and instruments have been considered as the DP Site project has evolved. However, a firm commitment to a given plan was delayed until recently to allow knowledge gained during the early phase of the evaluation to influence the decision.

Figure 34 shows the configuration to be implemented. Responsibilities for implementation have been assigned and firm dates for completion announced. System design has been completed and only a minor amount of instrument interface design remains.

We have defined information exchange protocols and communication interfaces. Operation sequences for technician/operators have been written. The external specification for the instrument-handling software has been agreed to and actual programming of this subsystem will begin in the near future.

2. DP Site Counting Room Activities (N. Baron)

Nondestructive assay of ^{240}Pu is routinely performed in the DP Site counting room by a comparison measurement using thermal-neutron coincidence counting techniques. Results of this measurement are used to calculate the effective mass of ^{240}Pu with the aid of the relation

$$M^u_{240}(\text{eff}) = \frac{N^u/\varepsilon^u}{N^{STD}/\varepsilon^{STD}} \sum_i \frac{a_i}{a_{240}} \frac{\bar{\nu}_i}{\bar{\nu}_{240}} M_i^{STD} , \quad (10)$$

where the effective mass of ^{240}Pu is defined to be

$$M^u_{240}(\text{eff}) \equiv \sum_i \frac{a_i}{a_{240}} \frac{\bar{\nu}_i}{\bar{\nu}_{240}} M_i^u . \quad (11)$$

In Eqs. 10 and 11 the summation is taken over the i isotopes of plutonium; N^u and N^{STD} are the true coincidence count rates for the spontaneous fission neutrons of the unknown and standard samples, respectively; a_i is the spontaneous fission rate per gram of isotope i; $\bar{\nu}_i$ is the number of prompt neutrons emitted per spontaneous fission event of a nucleus of isotope i; and ϵ^u and ϵ^{STD} are the coincident detection efficiencies for the spontaneous fission neutrons of the unknown and standard samples, respectively. The assumption is made that

$$\epsilon^u = \epsilon^{STD} . \quad (12)$$

This will be true if the matrix of the standard sample is chosen to be the same as that of the unknown sample.

The approximate total mass of plutonium is also obtained by the relation

$$M^u_{Pu} \approx \frac{M^u_{240}(\text{eff})}{f^u_{240}} , \quad (13)$$

where f^u_{240} is the best estimate of the isotopic abundance of ^{240}Pu in the unknown sample.

Heretofore the recording of all measurements and the subsequent calculations were done manually. However, recently the two neutron coincidence counting instruments in the DP Site counting room were linked to an on-line PDP-11 computer. This computer and its associated teletype terminal presently are located adjacent to the counting instruments (see Fig. 35). (Safeguards considerations dictate that in the future the computer will be inaccessible to the operator of the counting equipment.)

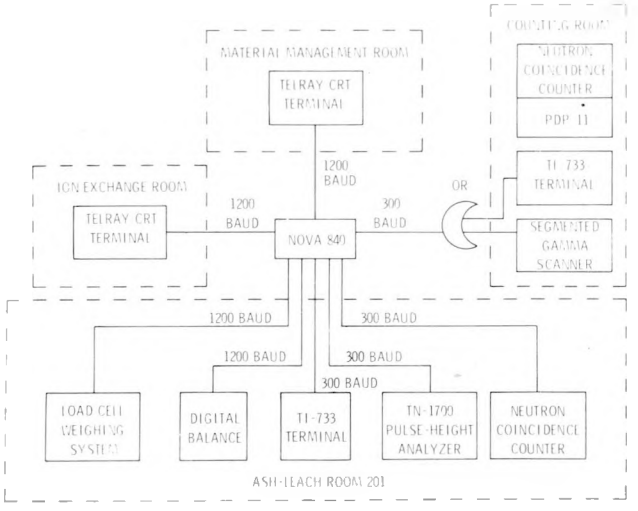

Fig. 34.
DYMAC configuration to be installed at DP Site.

Such a computerized system can (a) ultimately ensure detection of any attempt to tamper with the counting equipment and (b) significantly reduce the frequency of errors that can be expected when manually performing NDA analyses.

The software is designed to transmit instructions via common terminal to any measuring instrument linked to the computer regardless of the status of other instruments which are also computer-coupled. For example, other coupled instruments may be waiting to be activated, or they may be counting, or perhaps the computer is analyzing data following a counting run in one of these instruments.

Instructions are given by responding to programmed questions which are initiated by typing either RUN or an interrupt command at the teletype keyboard. These questions and their programmed responses are given in Table XV.

After the last question is answered, program execution begins automatically. If the answer to question 2 is YES, then all of the data and resultant analyses for all prior runs during that day will be listed in a compact tabular format by the computer. This feature is intended to serve as a hard-copy summary of the day's measurements made prior to this listing request. However, if the response to question 2 is NO, then the instrument's scalers are reset to zero and subsequently activated to count the sample identified by the response to question 3.

Following each run a listing is made automatically of the sample ID, date, counting instrument used, and result of the NDA analysis. This printout is attached to the assayed sample's container.

3. In-Line Neutron Coincidence Unit (N. Baron and R. Siebelist)

The in-line thermal-neutron coincidence counter (previously reported in Ref. 14, p. 16) is being installed in the ash-leach process system in Room 201 at DP Site. Photographs of its installation at various stages of completion are shown in Figs. 36-38. System calibration is currently in progress.

4. Solution Assay Instrument Evaluation (R. S. Marshall, W. R. Severe, J. L. Parker, and R. Siebelist, E. R. Martin)

An initial program to evaluate the SAI for the assay of 0.5- to 5.5-g/ℓ ash-leach solutions has been completed. Samples from 18 batches of ash-leach solutions have been assayed in the SAI. A portion of each sample was sent to Group CMB-1 for comparative assay via isotopic dilution mass spectroscopy.

After an initial set of samples was measured, it became apparent that the volumetric dispensing of 30.0-mℓ aliquots of the ash-leach solutions into the

TABLE XV

TERMINAL QUESTIONS AND RESPONSES

Question Number	Programmed Questions	Acceptable Responses
1	UNIT NUMBER (2, 3) READY?	2 or 3
2	DO YOU NOW WANT A LISTING OF ACCUMULATED DATA?	YES or NO
3	SAMPLE I.D.?	(any 9-character string)
4	IS THIS A STANDARD?	YES or NO
5	PERCENT ISOTOPIC ABUNDANCE OF Pu-240?	(any number)

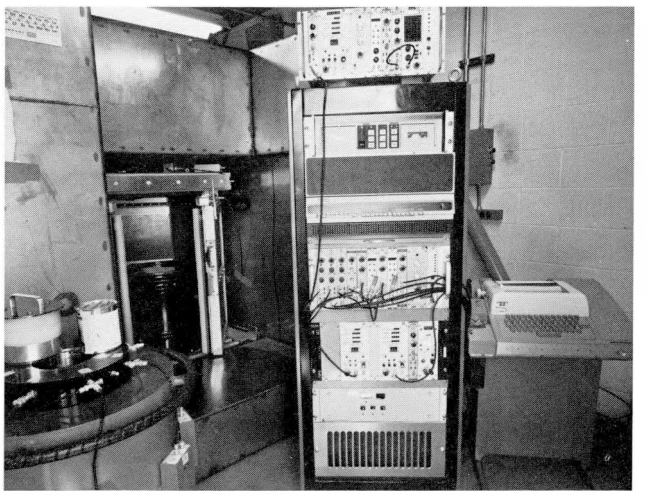

Fig. 35.
The PDP-11 computer and associated terminal control two independent neutron counting instruments.

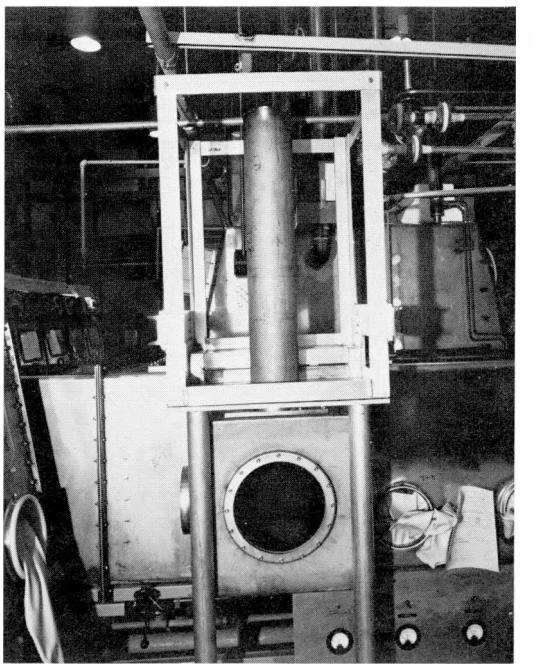

Fig. 36.
Installed glovebox well and support stand.

Fig. 37.
The 15 ^{3}He tubes supported by the high-voltage distribution junction box are being lowered into the moderator. The cadmium liner about the moderator and the partially stacked polyethylene shield are also shown.

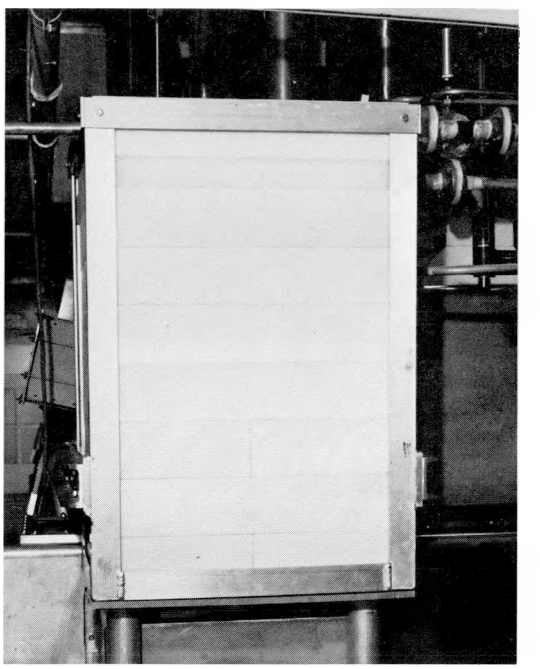

Fig. 38.
Completed assembly of the in-line thermal-neutron coincidence counter.

SAI measurement bottles was imprecise and biased. To circumvent this problem, the volume of each sample was determined from the sample net weight and specific gravity.

Table XVI lists the SAI and isotopic dilution assay results for each sample plus the ratios of the assays. The standard deviation for the ratio is 0.013 on a mean value of 0.981. Better agreement between the two methods was expected, thus an error analysis was performed on: the isotopic dilution mass spectroscopic method in total, specific gravity determination, sample weighing, and counting statistics. The first three measurements were tested by replicate measurements whereas the counting statistics error was calculated from sample and calibration standards counting data (refer to Table XVII).

Propagation of these error components yields a total error of 1.55%. Comparing this propagated error with observed data pair error of 1.33%, one can draw two conclusions:

(a) The SAI and isotopic dilution mass spectroscopic assays of the same samples agree within the propagated uncertainties of the two techniques.

(b) Precision improvements will be necessary to both assay techniques to ascertain whether the SAI meets the one standard deviation design criteria of 0.5% accuracy.

B. DYMAC for the New LASL Plutonium Facility

1. DYMAC Instrumentation (R. S. Marshall)

The first floor of the new LASL plutonium facility (TA-55) will have four process areas: ^{239}Pu R & D (100 Area), ^{238}Pu R & D (200 Area), metal fabrication (300 Area), and recycle (400 Area). Figure 39 shows the layout of the areas with their conveyor systems, and gives the general function of the rooms in each area.

Each area has been divided into unit processes and detailed studies have been made of glovebox usage. Once material flow, type, and packaging were established for each unit process, appropriate NDA instruments could be selected for all unit process inputs and outputs. Studies of material flow between unit processes suggest optimal placement of NDA instruments. Most of the instruments will be located in drop boxes, i.e., gloveboxes located immediately beneath the conveyor line and containing a raising and lowering mechanism for transferring materials into and out of the conveyor. Locations for neutron counters, solution assay instruments, and interactive terminals have been established and are shown in Figs. 40-43 which show each process area in detail. Locations for weighing devices (balances and load cells) and tank-solution assay instruments, while shown, are not firmly established.

Table XVIII lists the types and approximate numbers of NDA instruments and terminals required for TA-55. Not included in this list are instruments presently in use at DP Site: calorimeters, segmented gamma scanner, barrel counter (neutron coincidence) and two low-level trash counters (MEGAS and PANCAKE). Some of these instruments will be tied into the DYMAC system.

The material management rooms are used to enter and remove SNM from glovebox lines via the conveyor system. Each material management room is equipped with a thermal-neutron coincidence counter to measure SNM entering or being bagged out of the glovebox system. Items which cannot be assayed in the thermal-neutron coincidence counters will be transferred to the counting room for assay.

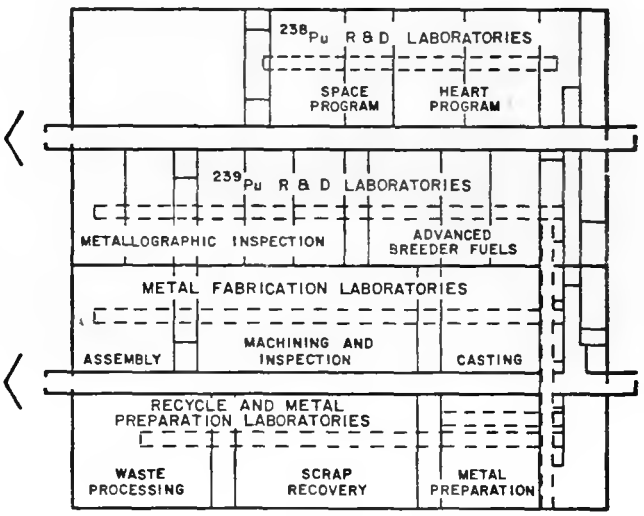

Fig. 39.
First floor plan of plutonium building. Overhead conveyors are indicated by dotted lines.

TABLE XVI

SAI VS ISOTOPIC DILUTION ASSAY OF ASH-LEACH SOLUTIONS

Sample Number	SAI Assay (plutonium g/ℓ)	Isotopic Dilution Assay (plutonium g/ℓ)	Ratio[a]
1	5.313	5.40	0.984
2	0.940	0.950	0.990
3	1.058	1.08	0.980
4	4.347	4.44	0.979
5	2.033	2.07	0.982
6	4.603	4.86	0.947
7	3.585	3.71	0.966
8	3.520	3.579	0.986
9	2.488	2.55	0.976
10	2.511	2.55	0.985
11	2.665	2.68	0.994
12	2.676	2.755	0.971
13	1.173	1.166	1.006
14	0.539	0.553	0.975
15	1.335	1.352	0.988
16	1.346	1.379	0.976
17	0.663	0.678	0.977
18	1.008	1.017	0.991

[a]SAI value divided by isotopic dilution value.

TABLE XVII

ERROR ANALYSIS

Error Component	Relative Standard Deviation (%)
Isotopic dilution mass spectroscopy	0.95
Specific gravity determination	0.22
Sample weighing	0.13
Counting statistics	1.20

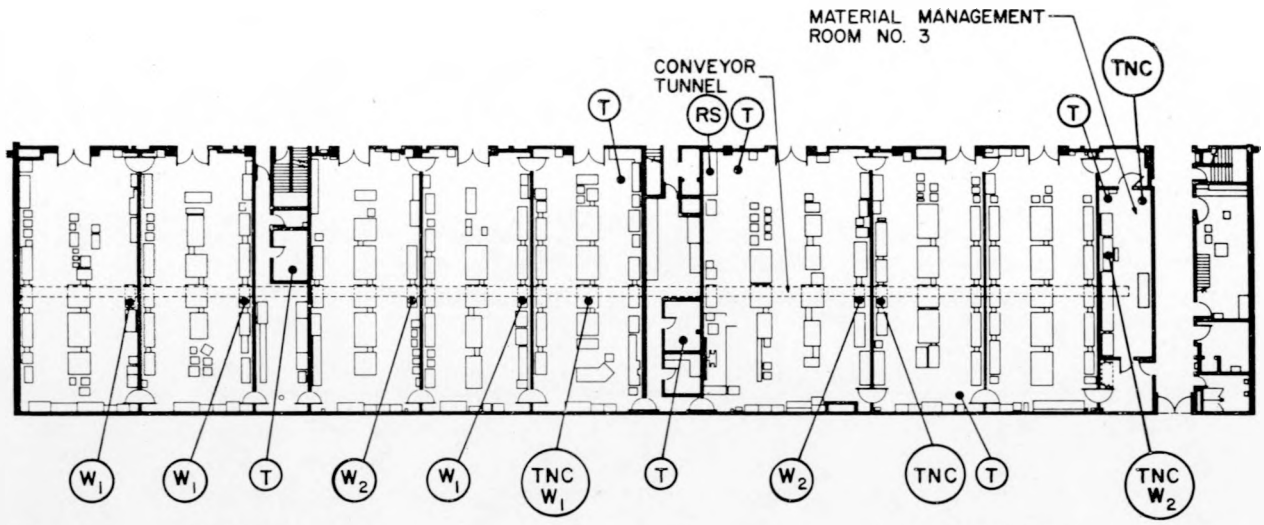

RS	Rod scanner	W_1	Balance, 0-200-2000 g
T	Interactive terminal	W_2	Balance, 0-10 000 g
TNC	Thermal-neutron coincidence counter		

Fig. 40.
Proposed DYMAC instrumentation for the R & D ^{239}Pu wing.

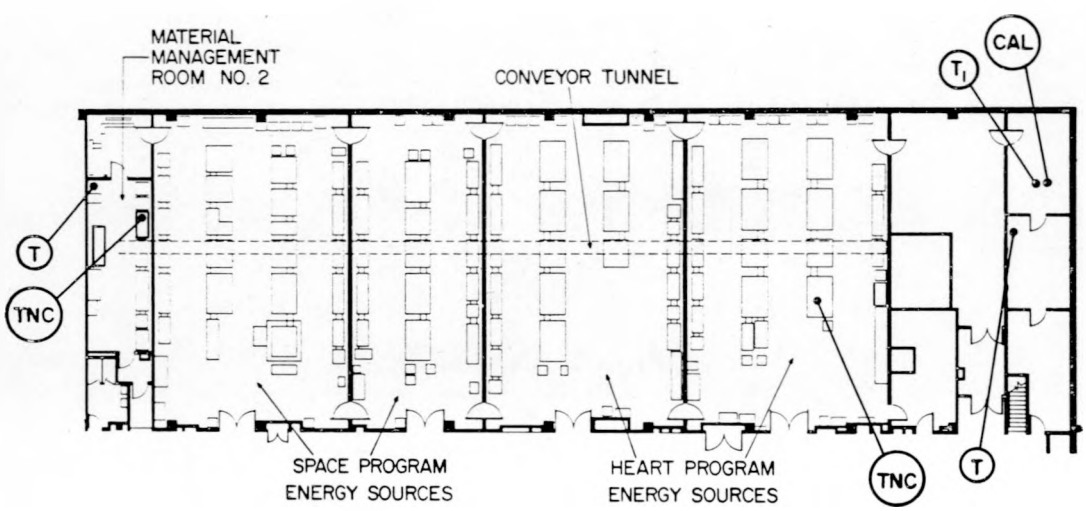

CAL	Calorimeter	T	Interactive terminal, floor model
T_1	Interactive terminal, supervisory model	TNC	Thermal-neutron coincidence counter

Fig. 41.
Proposed DYMAC instrumentation for the R & D ^{238}Pu wing.

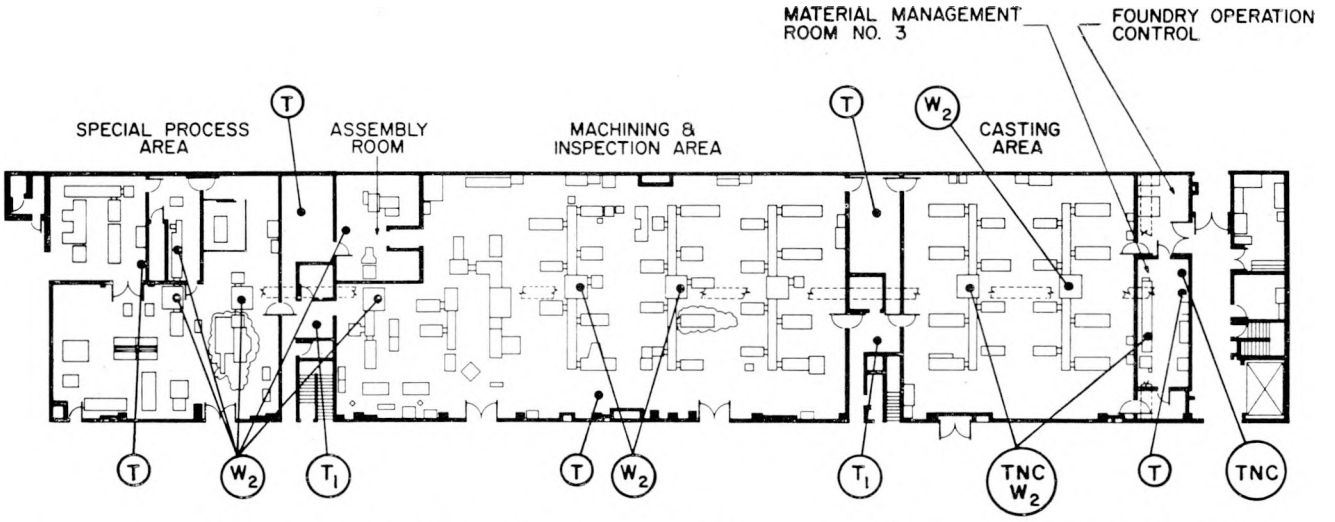

T	Interactive terminal, floor model	TNC	Thermal-neutron coincidence counter
T_1	Interactive terminal, supervisory model	W_2	Balance, 0-10 000 g

Fig. 42.

Proposed DYMAC instrumentation for the metal fabrication wing.

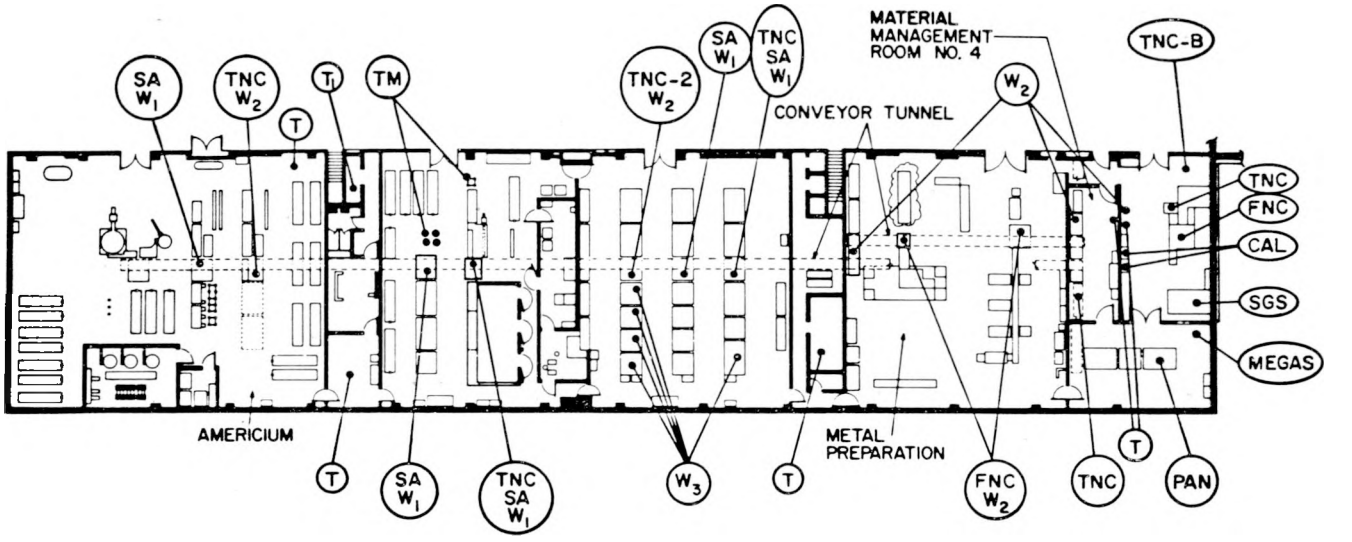

FNC	Fast-neutron coincidence counter	TNC	Thermal-neutron coincidence counter
MEGAS	Multienergy gamma scanner	TNC-2	TNC, low range (1-50 g of plutonium)
PAN	Pancake counter	TNC-B	TNC for barrels
SA	Solution assay instrument	W_1	Electronic balance, 0-200-2 000 g
SGS	Segmented gamma scanner	W_2	Electronic balance, 0-10 000 g
T	Interactive terminal, floor model	W_3	Load cells
T_1	Interactive terminal, supervisory model	TM	Tank measurement, gamma or x ray

Fig. 43.

Proposed DYMAC instrumentation for the recycle wing.

TABLE XVIII

DYMAC INSTRUMENTS AND TERMINALS FOR TA-55

Instrument or Terminal Type	Number Required			
	100 Area	200 Area	300 Area	400 Area
Thermal-neutron coincidence counter	4	2	3	5
Fast-neutron coincidence counter	0	0	0	2
Solution assay instrument	0	0	0	5
Interactive terminals	6	3	7	7
Balances	7	0	13	12
Load cells	0	0	0	6

Approximately 20% of the TA-55 gloveboxes have been received and are being installed. DYMAC instrument installations will require glovebox modification. Engineering drawings that specify the major modifications should be complete by October 1. Major glovebox modifications should begin during October and be complete some time in December.

2. Computer Procurement for TA-55 (R. F. Ford,* C. Slocomb,* and J. Hagen)

The necessary approval procedures have been initiated for procurement of the computer hardware and software necessary to implement DYMAC at TA-55.

A system study and a feasibility study were written and approved. Specifications were written and requests for bids sent to vendors. The bids were received, evaluated, and a prospective vendor selected. A computer justification study was written and has been submitted to the Albuquerque Operations Office (ALOO) for approval. The proposed contract has been submitted to the LASL Contract Review Board for approval. The purchase order will be placed within 2 weeks after the above apppovals with delivery expected 30-60 days later.

The hardware configuration will be as follows.

(a) Central processor: Eclipse C/330 (Data General), 128k 16-bit words.

(b) Input/output devices: system CRT terminal with two 5-million word disks, two 9-track tape units, and one 600-line-per-minute line printer.

(c) Communication provision: 128-line programmable multiplexor with current loop interfacing.

Group E-5.

III. TECHNOLOGY TRANSFER
(R. H. Augustson)

Presentations describing the LASL safeguards program were given at the Toronto meeting of the American Nuclear Society and the Annual Institute of Nuclear Materials Management Meeting held in Seattle.[42-44] These conference presentations allow Group R-1 to acquaint the entire safeguards community with recent advances made in its safeguards program.

Group R-1 hosted 60 visitors during the reporting period. Visitors attended group seminars, met individually with group members, viewed the installations at DP Site and TA-55, and gave a presentation of their organizations' activities. These visits permit an exchange of ideas, methods, and techniques with the visitors, and spread LASL safeguards technology.

Training began for process operators who will use interactive terminals as part of the DYMAC system at TA-55. Drawing on the experience gained from giving the sessions, a more formal program is being formulated.

REFERENCES

1. A. E. Evans, "The Expanding Role of the Small Van de Graaff in Nuclear Nondestructive Analysis," IEEE Trans. Nucl. Sci. **NS-20** (3), 989 (1973).

2. A. E. Evans and J. J. Malanify, "Nondestructive Assay of Inventory Verification Samples at the LASL Van de Graaff Small-Sample Assay Station," Nucl. Mater. Management **IV** (III), 309 (1975).

3. Nuclear Safeguards Research and Development Program Status Report, May-August 1970, Los Alamos Scientific Laboratory report LA-4523-MS (September 1970).

4. Nuclear Safeguards Research and Development Program Status Report, January-April 1971, Los Alamos Scientific Laboratory report LA-4705-MS (May 1971).

5. Nuclear Analysis Research and Development Program Status Report, January-April 1974, Los Alamos Scientific Laboratory report LA-5675-PR (August 1974).

6. Nuclear Analysis Research and Development Program Status Report, May-August 1972, Los Alamos Scientific Laboratory report LA-5091-PR (November 1972).

7. R. A. Forster, D. B. Smith, and H. O. Menlove, "Error Analysis of a ^{252}Cf Fuel-Rod-Assay System," Los Alamos Scientific Laboratory report LA-5317 (April 1974).

8. L. V. East and J. E. Swansen, "Charge-Sensitive Preamplifier for Use with Large Proportional Counter Arrays," Los Alamos Scientific Laboratory report LA-4972-MS (June 1972).

9. John Gray, Allied General Nuclear Services, private communication.

10. H. Goldstein, *Attenuation of Gamma Rays and Neutrons in Reactor Shields* (U. S. Atomic Energy Commission, Washington, DC, 1957).

11. C. J. Umbarger and L. R. Cowder, "Measurement of Transuranic Solid Wastes at the 10-nCi/g Activity Level," Los Alamos Scientific Laboratory report LA-5904-MS (March 1975).

12. Nuclear Analysis Research and Development Program Status Report, May-August 1973, Los Alamos Scientific Laboratory report LA-5431-PR (November 1973).

13. J. E. Glancy and E. L. Snooks, "In-Plant Evaluation of the NDA of HTGR Fuel," General Atomic Co. report GA-A13385 (June 1975).

14. Nuclear Safeguards Research Program Status Report, September-December 1975, Los Alamos Scientific Laboratory report LA-6316-PR (April 1976).

15. Nuclear Analysis Research and Development Program Status Report, January-April 1975, Los Alamos Scientific Laboratory report LA-6040-PR (August 1975).

16. Nuclear Safeguards Research Program Status Report, January-April 1976, Los Alamos Scientific Laboratory report LA-6530-PR (October 1976).

17. Nuclear Analysis Research and Development Program Status Report, September-December 1974, Los Alamos Scientific Laboratory report LA-5889-PR (April 1975).

18. G. Birkhoff, L. Bondar, and N. Coppo, "Variable Deadtime Neutron Counter for Tamper Resistant Measurements of Spontaneous Fission Neutrons," EUR-4801e, EURATOM, 1972.

19. R. Berg, G. Birkhoff, L. Bondar, G. Busca, J. Lev, and R. Swennen, "On the Determination of the ^{240}Pu in Solid Waste Containers by Spontaneous Fission Neutron Measurements. Application to Reprocessing Plant Waste," Eurochemic Technical report ETR-280 (1974).

20. M. M. Stephens, J. E. Swansen, and L. V. East, "Shift Register Neutron Coincidence Module," Los Alamos Scientific Laboratory report LA-6121-MS (November 1975).

21. C. H. Vincent, *Random Pulse Trains* (Peter Peregrinus, Ltd., London, 1973), pp. 100-102.

22. K. Böhnel, "Die Plutoniumbestimmung in Kernbrennstoffen mit der Neutronen Koinzidenzmethode," KFK2203, Karlsruhe (September 1975).

23. C. V. Strain and R. J. Omohundro, "Coincident Neutron Equipment," Naval Research Laboratory Memorandum report 2107 (1970).

24. E. Lopez-Menchero and A. J. Waligura, "The IAEA Programme for the Development of Safeguards Techniques and Instrumentation," Int. Symp. on the Safeguarding of Nuclear Materials, Vienna, October 20-24, 1975.

25. Nuclear Analysis Research and Development Program Status Report, May-August 1975, Los Alamos Scientific Laboratory report LA-6142-PR (December 1975).

26. D. R. Terrey and A. P. Dixon, "A Portable Gamma Absorptiometer for Safeguards Use in Nuclear Fuel Processing Plants. Final Report for the Period 1 December 1972 - 30 November 1973," International Atomic Energy Agency report IAEA-R-1308-F (1974).

27. W. H. McMaster, N. Kerr Del Grande, J. H. Mallett, and J. H. Hubbell, "Compilation of X-Ray Cross Sections," Univ. of California Lawrence Radiation Laboratory report UCRL-50174 (May 1969).

28. E. R. Martin, D. F. Jones, and L. G. Speir, "Passive Segmented Gamma Scan Operation Manual," Los Alamos Scientific Laboratory report LA-5652-M (July 1974).

29. T. R. Canada, J. L. Parker, and T. D. Reilly, "Total Plutonium and Uranium Determination by Gamma-Ray Densitometry," Am. Nucl. Soc. Trans. **22,** 140 (1975).

30. J. A. Bearden and A. F. Burr, "Reevaluation of X-Ray Atomic Energy Levels," Rev. Mod. Phys. **39,** 125 (1967).

31. W. J. Veigele, "Photon Cross Sections from 0.1 keV to 1 MeV for Elements Z = 1 to Z = 94," Atom. Data Tables **5,** 51 (1973).

32. R. L. Heath, "Gamma-Ray Spectrum Catalog: Ge(Li) and Si(Li) Spectrometry," Aerojet Nuclear Co. report ANCR-1000-2 (3rd Ed.) (March 1974).

33. O. Keski-Rahkonen and M. O. Krause, "Total and Partial Atomic-Level Widths," Atom. Nucl. Data Tables **14,** 139 (1974).

34. A. E. Sandström, "Experimental Methods of X-Ray Spectroscopy: Ordinary Wavelengths," Handbuck der Physik **XXX,** 78 (1957).

35. B. M. Kincaid and P. Eisenberger, "Synchrotron Radiation Studies of the K-Edge Photoabsorption Spectra of Kr, Br_2, and $GeCl_4$: A Comparison of Theory and Experiment," Phys. Rev. Lett. **34,** 1361 (1975).

36. F. K. Richtmeyer, S. W. Barnes, and E. Ramberg, "The Widths of the L-Series Lines and of the Energy Levels of Au(79)," Phys. Rev. **46,** 843 (1934).

37. A. E. Evans and M. S. Krick, "Equilibrium Delayed-Neutron Spectra from Fast Fission of ^{235}U, ^{238}U, and ^{239}Pu," submitted to Nucl. Sci. Eng.

38. W. R. Sloan and G. L. Woodruff, "Spectrum of Delayed-Neutrons from the Thermal-Neutron Fission of Uranium-235," Nucl. Sci. Eng. **55,** 28 (1974).

39. R. H. Augustson, T. D. Reilly, and T. R. Canada, "The LASL-U.S. ERDA Nondestructive Assay Training Program," Nucl. Mater. Management **V** (I), (1976).

40. American National Standards Institute, "Nondestructive Assay Measurement Control and Assurance, ANSI N15.36 draft, to be published.

41. J. P. Shipley, D. D. Cobb, R. J. Dietz, M. L. Evans, E. P. Schelonka, D. B. Smith, and R. B. Walton, "Coordinated Safeguards for Materials Management in a Mixed-Oxide Fuel Facility," Los Alamos Scientific Laboratory report LA-6536, to be published.

42. R. H. Augustson, "Development of In-Plant 'Real-Time' Materials Control—the DYMAC Program," Proc. Inst. Nucl. Mater. Management, 17th, Seattle, June 22-24, 1976, Vol. **V** (III), pp. 302-316.

43. J. M. deMontmollin and R. B. Walton, "The Design of Integrated Safeguards Systems for Nuclear Facilities," Proc. Inst. Nucl. Mater. Management, 17th, Seattle, June 22-24, 1976, Vol. **V** (III), pp. 317-332.

44. J. W. Tape, D. A. Close, and R. B. Walton, "Total Room Holdup of Plutonium Measured with a Large-Area Neutron Detector," Proc. Inst. Nucl. Mater. Management, 17th, Seattle, June 22-24, 1976, Vol. **V** (III), pp. 533-539.

PUBLICATIONS

M. S. Krick and A. E. Evans, "Equilibrium Delayed-Neutron Energy Spectra from Fast Fission of U-235, U-238, and Pu-239," Am. Phys. Soc. Meeting, Washington, DC, April 29, 1976.

J. L. Parker and T. D. Reilly, "Bulk Sample Self-Attenuation Correction by Transmission Measurement," ERDA Symp. on X- and Gamma-Ray Sources and Applications, Univ. of Michigan, Ann Arbor, May 19-21, 1976.

R. H. Augustson, "Development of In-Plant 'Real-Time' Materials Control—the DYMAC program," Proc. Inst. Nucl. Mater. Management, 17th, Seattle, June 22-24, 1976, Vol. **V** (III), pp. 302-316.

J. M. deMontmollin and R. B. Walton, "The Design of Integrated Safeguards Systems for Nuclear Facilities," Proc. Inst. Nucl. Mater. Management, 17th, Seattle, June 22-24, 1976, Vol. **V** (III), pp. 317-332.

J. W. Tape, D. A. Close, and R. B. Walton, "Total Room Holdup of Plutonium Measured with a Large-Area Neutron Detector," Proc. Inst. Nucl. Mater. Management, 17th, Seattle, June 22-24, 1976, Vol. Vol. **V** (III), pp. 533-539.

GLOSSARY

ALOO	Albuquerque Operations Office
ASCII	American standard code for information interchange
BCD	binary coded decimal
BWR	boiling water reactor
cusum	cumulative summation
DPM	digital panel meter
FFTF	fast flux test facility
IAEA	International Atomic Energy Agency
LED	light-emitting diode
LWR	light water reactor
MACSIM	Material Accounting and Control SIMulation
NDA	nondestructive assay
PBSW	pushbutton switches
PWR	pressurized water reactor
RC	resistor-capacitor
SAI	solution assay instrument
SGS	segmented gamma scanner
SNM	special nuclear material
SSAS	small sample assay station
TRU	transuranic
TTL	transistor-to-transitstor logic
VDC	variable deadtime counter

☆ U.S. GOVERNMENT PRINTING OFFICE 1977—777-018/16